Physica A 174 (1991) 355–390
North-Holland

FAR FROM EQUILIBRIUM VELOCITY DISTRIBUTION OF A DILUTE GAS

Andrés SANTOS
Departamento de Física, Universidad de Extremadura, E-06071 Badajoz, Spain

J. Javier BREY
Física Teórica, Universidad de Sevilla, Apdo 1065, E-41080 Sevilla, Spain

Received 25 September 1990

The one-particle distribution function of a dilute gas under uniform shear flow is investigated by means of the Bhatnagar–Gross–Krook (BGK) model kinetic equation. For repulsive interaction potentials of the form $V(r) \propto r^{-l}$ a hydrodynamic regime, characterized by a normal solution of the BGK equation, is identified in the proper limit, for arbitrary shear rates. This normal solution diverges at zero velocity, except for sufficiently small shear rates in the case of Maxwell molecules ($l = 4$). Besides, it becomes highly distorted as compared to local equilibrium.

1. Introduction

The statistical mechanical description of systems in states close to thermal equilibrium can be considered as a well established theory [1]. For example, the constitutive equations for heat and momentum fluxes of a simple fluid are known. In far from equilibrium situations, however, the problem is much more complicated and a large number of questions still remain open. In particular, the constitutive relations must be generalized to include a nonlinear dependence on the hydrodynamic gradients [2]. Despite the lack of fundamental theoretical advances, a large number of nonequilibrium computer simulations have been carried out [3], some of them without a sound justification [4, 5].

The prototype system for the study of transport properties is a monatomic, dilute gas with short-range interaction. Instead of a fully statistical mechanical description in terms of the phase-space probability density, it is much more convenient to adopt a kinetic description, according to which the state of the system is characterized by the one-particle velocity distribution function (VDF) $f(\boldsymbol{r}, \boldsymbol{v}; t)$. Its first five velocity moments give the local densities of conserved quantities:

$$n(\boldsymbol{r}, t) = \int \mathrm{d}\boldsymbol{v}\, f(\boldsymbol{r}, \boldsymbol{v}; t)\,, \tag{1.1}$$

$$n(\boldsymbol{r}, t)\, \boldsymbol{u}(\boldsymbol{r}, t) = \int \mathrm{d}\boldsymbol{v}\, \boldsymbol{v} f(\boldsymbol{r}, \boldsymbol{v}; t)\,, \tag{1.2}$$

$$\tfrac{3}{2} n(\boldsymbol{r}, t)\, k_{\mathrm{B}} T(\boldsymbol{r}, t) = \int \mathrm{d}\boldsymbol{v}\, \tfrac{1}{2} m[\boldsymbol{v} - \boldsymbol{u}(\boldsymbol{r}, t)]^2 f(\boldsymbol{r}, \boldsymbol{v}; t)\,, \tag{1.3}$$

where n, $\boldsymbol{u}$, and T are the local number density, velocity and temperature, respectively. In eq. (1.3), m is the mass of a particle and k_{B} is the Boltzmann constant. The next moments of f provide the fluxes, such as the pressure tensor

$$P_{ij}(\boldsymbol{r}, t) = \int \mathrm{d}\boldsymbol{v}\, m[v_i - u_i(\boldsymbol{r}, t)][v_j - u_j(\boldsymbol{r}, t)] f(\boldsymbol{r}, \boldsymbol{v}; t)\,. \tag{1.4}$$

In a dilute gas, the evolution equation for the VDF is the Boltzmann equation (BE), which in standard notation reads [6]

$$\frac{\partial f}{\partial t} + \boldsymbol{v} \cdot \nabla f = \int \mathrm{d}\boldsymbol{v}_1 \int \mathrm{d}\Omega\, |\boldsymbol{v} - \boldsymbol{v}_1| \sigma_{\mathrm{s}}(|\boldsymbol{v} - \boldsymbol{v}_1|, \theta)\, (f' f_1' - f f_1)\,. \tag{1.5}$$

For a given specific problem, this equation must be solved subject to appropriate initial and boundary conditions. Nevertheless, for times much longer than the mean free time and for distances from the walls much larger than the mean free path, one expects the system to reach a hydrodynamic regime. In that regime, the BE is expected to admit a (so-called) normal solution, in which f depends on $\boldsymbol{r}$ and t only through a functional dependence on the hydrodynamic fields: n, $\boldsymbol{u}$ and T. The usual method to construct normal solutions to the BE is provided by the Chapman–Enskog (CE) theory [7], which is based on an expansion of the VDF in powers of gradients of the hydrodynamic fields. From a practical point of view, however, the usefulness of the CE method is restricted to the first few terms (Navier–Stokes and Burnett orders) [6, 8].

As said before, several important questions arise in the study of transport in far from equilibrium situations. In this paper. we shall be mainly concerned with (i) the existence of a time-dependent normal solution beyond the scope of the first few terms in the CE expansion, (ii) the character (asymptotic versus convergent) of the CE series, (iii) the distortion of the VDF far from equilibrium, and (iv) the influence on the above points of the interaction potential under consideration.

Due to the wide diversity of possible nonequilibrium situations, we shall restrict ourselves to the well-known state of uniform shear flow (USF). This state has received much attention in simulation [3, 9, 10] as well as in theoretical studies [4, 5, 11–13]. At a macroscopic level, the USF is character-

ized by a linear profile of the x-component of the local velocity along the y-axis, a constant density, and a uniform temperature:

$$u_i = a_{ij} r_j , \qquad a_{ij} = a\delta_{ix}\delta_{jy} , \qquad a = \text{const.} , \tag{1.6a}$$

$$n = \text{const.} , \tag{1.6b}$$

$$\nabla T = \mathbf{0} . \tag{1.6c}$$

One of the advantages of this state is that fourteen of the possible hydrodynamic gradients are zero, the only nonzero gradient $(\partial u_x/\partial y)$ being a constant. Moreover, there are no boundary effects, due to the absence of moving mechanical walls. These advantages are counterbalanced by the fact that the total energy does not remain constant, so that the temperature monotonically increases in time. Although external drag forces have been proposed to account for this viscous heating and get a stationary state [3], they do not seem to play a neutral role [4, 5] and, therefore, they will be omitted in this work. This time dependence of the USF, including the existence of an initial layer, renders the problem most interesting.

To the best of our knowledge, the only exact results obtained from the BE for the USF refer to the case of Maxwell molecules [13–15]. For other interaction potentials, one must resort to simulation [10]. Even in the case of Maxwell molecules, information about the VDF is obtained only indirectly through the knowledge of a finite number of its moments. Consequently, in order to address the points quoted above, it is convenient to use the Bhatnagar–Gross–Krook (BGK) kinetic equation [16] as a model of the BE. In this model, the Boltzmann collision operator is replaced by a single-time relaxation towards the local equilibrium distribution:

$$\frac{\partial f}{\partial t} + \boldsymbol{v}\cdot\nabla f = -\zeta(f - f_{\mathrm{LE}}) , \tag{1.7}$$

where

$$f_{\mathrm{LE}}(\boldsymbol{r}, \boldsymbol{v}; t) = n(\boldsymbol{r}, t)\left(\frac{m}{2\pi k_{\mathrm{B}} T(\boldsymbol{r}, t)}\right)^{3/2} \exp\left(-\frac{m}{2k_{\mathrm{B}} T(\boldsymbol{r}, t)}[\boldsymbol{v} - \boldsymbol{u}(\boldsymbol{r}, t)]^2\right) \tag{1.8}$$

is the local equilibrium VDF and $\zeta(\boldsymbol{r}, t)$ is an effective collision frequency, which depends on position and time through the local density and temperature. The only influence of the interaction potential enters into the BGK equation through the temperature-dependence of the collision frequency. In a dilute gas,

ζ is just linear in n. Its dependence on T is much less trivial. The simplest case corresponds to purely repulsive potentials of the form $V(r) \sim r^{-l}$. Then, dimensional analysis shows that

$$\zeta = AnT^{\alpha}, \qquad \alpha \equiv 1/2 - 2/l, \tag{1.9}$$

where A depends on k_B, m and the potential coefficient, but is otherwise a constant. In the particular case of Maxwell molecules ($l = 4$), $\alpha = 0$, and the collision frequency becomes independent of the temperature. On the other hand, $\alpha = 1/2$ for hard spheres ($l \to \infty$) and ζ grows then with the square root of the temperature. In the following, we shall restrict ourselves to collision frequencies given by eq. (1.9), considering $\alpha = 0$ and $\alpha = 1/2$ as limit cases.

The BGK equation keeps the main physical properties of the BE, namely the conservation of mass, momentum and energy, and also the verification of an H-theorem [16]. Recent simulations in dilute gases show the relevance of the BGK predictions, even at a quantitative level, for states far from equilibrium [10, 17]. As we shall see, the combined simplicity of the USF state and the BGK equation allows one to analyze with some detail the properties of nonequilibrium states.

The organization of this paper is as follows. In section 2, the general solution to the BGK equation for a gas under USF is obtained and analyzed. In the especial case of Maxwell molecules (section 3), the general solution is easily seen to become a normal solution as time progresses. The corresponding VDF exhibits some unexpected features for shear rates beyond a certain threshold value. More general potentials are considered in section 4. The time-dependence of the collision frequency gives rise to mathematical and conceptual problems much more involved than in the case of constant collision frequency (Maxwell molecules). As a consequence, a normal state in a strong sense, i.e. after a large number of effective collisions per particle, is restricted to local equilibrium. However, a far from equilibrium normal state can be identified if the weaker condition of waiting until the temperature has increased by a large factor is adopted. The conclusions are summarized and discussed in section 5.

2. General solution of the BGK equation for USF

The problem we face is to find a solution to the BGK equation, eqs. (1.7) and (1.8), that is consistent with the USF state, eqs. (1.6). If the initial condition verifies eqs. (1.6), the consistency between eqs. (1.6) and (1.7) is satisfied by imposing generalized periodic boundary conditions. It is convenient to introduce the position $\boldsymbol{R}$ and the velocity $\boldsymbol{V}$ with respect to a frame moving

with the flow velocity:

$$R_i = \Lambda_{ij}(t)\, r_j\,, \qquad \Lambda_{ij}(t) \equiv \delta_{ij} - a_{ij} t\,, \tag{2.1}$$

$$V_i = v_i - a_{ij} r_j\,. \tag{2.2}$$

Eq. (1.7) can then be rewritten as

$$\frac{\partial \bar{f}}{\partial t} + \Lambda_{ij}(t)\, V_j \frac{\partial \bar{f}}{\partial R_i} - a_{ij} V_j \frac{\partial \bar{f}}{\partial V_i} = -\zeta(\bar{f} - \bar{f}_{\mathrm{LE}})\,, \tag{2.3}$$

where $\bar{f}(\boldsymbol{R}, \boldsymbol{V}; t) \equiv f(\boldsymbol{r}, \boldsymbol{v}; t)$. At a macroscopic level, the USF is spatially uniform in this Lagrangian frame. This implies that the local equilibrium VDF $\bar{f}_{\mathrm{LE}}$ is also uniform,

$$\bar{f}_{\mathrm{LE}}(\boldsymbol{V}, t) = n\left(\frac{m}{2\pi k_{\mathrm{B}} T(t)}\right)^{3/2} \exp\left(-\frac{mV^2}{2k_{\mathrm{B}} T(t)}\right). \tag{2.4}$$

If we restrict ourselves to uniform initial distributions $\bar{f}(\boldsymbol{V}, t_0)$, then eq. (2.3) preserves this spatial uniformity in time, so that it misses the second term in the left side and reduces to

$$\frac{\partial f}{\partial t} - a_{ij} V_j \frac{\partial f}{\partial V_i} = -\zeta(f - f_{\mathrm{LE}})\,, \tag{2.5}$$

where we have dropped the bar on $f(\boldsymbol{V}, t)$. Notice that eq. (2.5) is invariant under the transformations $(V_x, V_y, V_z) \leftrightarrow (V_x, V_y, -V_z) \leftrightarrow (-V_x, -V_y, V_z)$.

It is straightforward to get from eq. (2.5) the following closed set of equations:

$$\frac{\partial}{\partial t} P_{ij} + (a_{ik} P_{jk} + a_{jk} P_{ik}) = -\zeta(P_{ij} - p\delta_{ij})\,, \tag{2.6}$$

where P_{ij} is the pressure tensor defined by eq. (1.4) and $p = \frac{1}{3} P_{ii} = n k_{\mathrm{B}} T$ is the hydrostatic pressure. In particular,

$$\frac{\partial}{\partial t} p = -\tfrac{2}{3}\, a P_{xy}\,, \tag{2.7}$$

$$\frac{\partial}{\partial t} P_{xy} = -\zeta P_{xy} - a P_{yy}\,, \tag{2.8}$$

$$\frac{\partial}{\partial t} P_{yy} = -\zeta P_{yy} + \zeta p\,. \tag{2.9}$$

Since P_{yy} is positive definite, it follows from eq. (2.8) that if P_{xy} were positive at a certain time, it would decrease monotonically until becoming negative, which is the physically meaningful sign. Thus, according to eq. (2.7), the temperature monotonically increases in time (except, perhaps, for a short initial period of time). In general, this viscous heating has an important influence on the average collision rate, which will increase with time according to eq. (1.9). An exception is the case of Maxwell molecules, where the rate at which collisions take place remains constant.

The general solution of eq. (2.5) is

$$f(\boldsymbol{V}, t) = \exp(-s) \exp[(t - t_0) a_{ij} V_j \partial/\partial V_i] f(\boldsymbol{V}, t_0) + \int_{t_0}^{t} \mathrm{d}t' \, \zeta(t') \exp[-(s - s')] \exp[(t - t') a_{ij} V_j \partial/\partial V_i] f_{\mathrm{LE}}(\boldsymbol{V}, t') , \tag{2.10}$$

where $t_0 < t$ is the initial time,

$$s(t) = \int_{t_0}^{t} \mathrm{d}t' \, \zeta(t') \tag{2.11}$$

is the average number of collisions per particle between t_0 and t, $s' \equiv s(t')$, and $\exp(t a_{ij} V_j \partial/\partial V_i)$ is a shift operator:

$$\exp(t a_{ij} V_j \partial/\partial V_i) \, g(\boldsymbol{V}) = g(\boldsymbol{\Lambda}(-t) \cdot \boldsymbol{V}) . \tag{2.12}$$

In order to have an explicit solution, one must proceed as follows. Given the initial VDF $f(\boldsymbol{V}, t_0)$, one gets the initial values $p(t_0)$, $P_{xy}(t_0)$ and $P_{yy}(t_0)$. By solving the set (2.7)–(2.9), where $\zeta \propto p^{\alpha}$, the temperature $T(t)$, $t > t_0$, is obtained. Its knowledge, along with that of $s(t)$, allows one to obtain $f(\boldsymbol{V}, t)$ at any desired time $t > t_0$.

In transport phenomena, however, one is not mainly interested in the time evolution of the VDF corresponding to a specific initial condition. As discussed in the introduction, it is expected that, after a certain transient period, the VDF reaches a form in which all the space and time dependence occurs through the hydrodynamic fields (n, $\boldsymbol{u}$ and T), the functional dependence being independent of the initial conditions. Such a VDF is called a normal solution to the kinetic equation, and holds in the so-called hydrodynamic stage of the temporal evolution. The existence of a normal solution also requires to consider points far enough from the boundaries of the system. Since those boundaries do not exist in the USF, we can concentrate on the initial layer.

The standard method to construct the normal solution is the Chapman–Enskog method [6, 7]. Although quite general and elegant, this method is restricted, at least from a practical point of view, to states close to equilibrium. In order to investigate the possible existence of normal solutions far from equilibrium, it is better to consider particular simple states as illustrative examples. The USF is a suitable time-dependent state affording a detailed analysis.

In order to explore the possible existence of a hydrodynamic regime, it is convenient to introduce dimensionless quantities. A natural velocity scale is defined by the temperature

$$V^* \equiv [2k_B T(t)/m]^{-1/2} V . \tag{2.13}$$

Accordingly, the reduced VDF is defined as

$$f^* \equiv \frac{1}{n} [2k_B T(t)/m]^{3/2} f . \tag{2.14}$$

The remnant time dependence, as well as the parametric dependence on the shear rate a, is accounted for through the reduced shear rate

$$a^* \equiv a/\zeta(t) . \tag{2.15}$$

The physical meaning of a^* is evident. It represents a uniformity parameter, namely the ratio between the mean free path and a characteristic hydrodynamic length. In other words, a^* is the only relevant parameter measuring the deviation from equilibrium. When applying the Chapman–Enskog method to the USF, a^* turns out to be the dimensionless expansion parameter.

Notice that for every initial condition $f(V, t_0)$ we have a VDF $f(V, t)$ that can be mapped onto the corresponding $f^*(V^*; a^*)$. Consequently, there exists in principle a different $f^*(V^*; a^*)$ for every $f(V, t_0)$. Nevertheless the existence of a normal solution to the kinetic equation means that $f^*(V^*; a^*)$ must reach in the long-time limit ($t - t_0 \to \infty$) a well defined form independent of the initial conditions. If that limit is understood in the strongest sense, a rather trivial result arises. Due to viscous heating, the collision frequency increases in time, except in the case of Maxwell molecules (where $\zeta = \text{const.}$). Thus, $a^* \to 0$ when $t - t_0 \to \infty$ and the normal VDF becomes the local equilibrium one. According to this, a far from equilibrium normal solution would be only meaningful in the case of Maxwell molecules. As we shall see, that is not the case. The task of obtaining the normal $f^*(V^*; a^*)$ from the general solution (2.10) will be carried out in section 3 for Maxwell molecules and in section 4 for more general interaction potentials.

Before closing this section, notice that the definitions (2.13) and (2.14) imply the following normalization conditions:

$$\int \mathrm{d}\boldsymbol{V}^* \, f^*(\boldsymbol{V}^*; a^*) = 1 , \tag{2.16}$$

$$\int \mathrm{d}\boldsymbol{V}^* \, \boldsymbol{V}^* f^*(\boldsymbol{V}^*; a^*) = 0 , \tag{2.17}$$

$$\int \mathrm{d}\boldsymbol{V}^* \, V^{*2} f^*(\boldsymbol{V}^*; a^*) = \tfrac{3}{2} . \tag{2.18}$$

Since the VDF $f^*(\boldsymbol{V}^*; a^*)$ depends on the three components of $\boldsymbol{V}^*$, it is useful to introduce some marginal distributions functions. We define

$$\tilde{f}^*(V_x^*, V_y^*; a^*) \equiv \int_{-\infty}^{\infty} \mathrm{d}V_z^* \, f^*(\boldsymbol{V}^*; a^*) , \tag{2.19}$$

$$F_x^{(+)}(V_x^*; a^*) \equiv \int_0^{\infty} \mathrm{d}V_y^* \, \tilde{f}^*(V_x^*, V_y^*; a^*) , \tag{2.20}$$

$$F_y^{(+)}(V_y^*; a^*) \equiv \int_0^{\infty} \mathrm{d}V_x^* \, \tilde{f}^*(V_x^*, V_y^*; a^*) . \tag{2.21}$$

3. Maxwell molecules

In the case of Maxwell molecules, the collision frequency remains constant, since $\alpha = 0$ in eq. (1.9). Consequently, the only effect of viscous heating is to increase the thermal velocity without modification of the rate of collisions. In particular, the reduced shear rate $a^* = a/\zeta$ is a constant, so that the "distance" of the system from equilibrium does not change in time.

From a mathematical point of view, the fact that $\zeta = \text{const.}$ makes the set of equations (2.7)–(2.9), or equivalently the closed third order differential equation

$$\left(\frac{\partial}{\partial t} + \zeta\right)^2 \frac{\partial}{\partial t} \, p = \tfrac{2}{3} a^2 \zeta p , \tag{3.1}$$

linear. It is worth mentioning that eqs. (2.7)–(2.9) and (3.1) also hold in the context of the BE for Maxwell molecules under USF, ζ being then related to an eigenvalue of the linearized BE [13, 15]. The general solution of eq. (3.1) is

$$p(t) = C_1 \exp(\lambda t) + \exp(\mu t)\,(C_2 \cos \omega t + C_3 \sin \omega t)\,, \tag{3.2}$$

where λ and $\mu \pm i\omega$ are the roots of the characteristic equation

$$\lambda^*(1+\lambda^*)^2 = \tfrac{2}{3}a^{*2}\,, \qquad \lambda^* \equiv \lambda/\zeta\,. \tag{3.3}$$

More explicitly,

$$\begin{aligned}\lambda &= \tfrac{4}{3}\zeta\, \mathrm{sh}^2[\tfrac{1}{6}\,\mathrm{ch}^{-1}(1+9a^{*2})] \\ &= \tfrac{1}{3}\zeta[(1+9a^{*2}+3\sqrt{2a^{*2}+9a^{*4}})^{1/3} \\ &\quad + (1+9a^{*2}-3\sqrt{2a^{*2}+9a^{*4}})^{1/3}-2]\,,\end{aligned} \tag{3.4}$$

$$\mu = -(\tfrac{1}{2}\lambda + \zeta)\,, \tag{3.5}$$

$$\omega = [\lambda(\tfrac{3}{4}\lambda + \zeta)]^{1/2}\,. \tag{3.6}$$

The constants C_1, C_2 and C_3 are determined by the initial values $p(t_0)$, $P_{xy}(t_0)$ and $P_{yy}(t_0)$. The first term in the right side of eq. (3.2) grows in time, while the second term decreases. Thus, for $\zeta t \gg 1$,

$$p(t) = C_1 \exp(\lambda t)\,. \tag{3.7}$$

By inserting this into eq. (2.6) and using eq. (3.3), one can see that the reduced pressure tensor $P_{ij}^* \equiv P_{ij}/p$ asymptotically reaches the following steady values:

$$P_{xy}^* = -\frac{3}{2}\frac{\lambda^*}{a^*}\,, \tag{3.8}$$

$$P_{yy}^* = P_{zz}^* = (1+\lambda^*)^{-1}\,, \tag{3.9}$$

$$P_{xz}^* = P_{yz}^* = 0\,, \tag{3.10}$$

where $\lambda^* \equiv \lambda/\zeta$. Notice that eqs. (3.8)–(3.10) hold for arbitrary initial conditions in the long-time limit, so that they clearly correspond to the normal solution of the kinetic equation. It might seem that an exception corresponds to a particular initial condition for which $C_1 = 0$. But such an initial condition is incompatible with a positive definite VDF, since then $p(t)$ would take negative values for time periods of length π/ω. From eqs. (3.8) and (3.9) one can get expressions for the generalized shear viscosity,

$$\eta^*(a^*) \equiv -\frac{P_{xy}^*}{a^*} = \frac{3}{2}\frac{\lambda^*}{a^{*2}} = \frac{2}{a^{*2}}\,\mathrm{sh}^2[\tfrac{1}{6}\,\mathrm{ch}^{-1}(1+9a^{*2})]\,, \tag{3.11}$$

and viscometric functions,

$$\Psi_1(a^*) \equiv \frac{P_{yy}^* - P_{xx}^*}{a^{*2}} = -2(1+\lambda^*)^{-3}\,, \tag{3.12}$$

$$\Psi_2(a^*) \equiv \frac{P_{zz}^* - P_{yy}^*}{a^{*2}} = 0\,. \tag{3.13}$$

These are the main transport coefficients in this problem. The quantity λ^* is a function of $z \equiv a^{*2}$. The only singularity for finite z is a branch point at $z = -2/9$. In particular, the origin $z = 0$ is a regular point, which implies that the expansions of λ^*, η^* and Ψ_1 in powers of z converge for $|z| < 2/9$. The first few terms are

$$\lambda^* = \tfrac{2}{3}(z - \tfrac{4}{3}z^2 + \tfrac{28}{9}z^3 + \cdots)\,, \tag{3.14}$$

$$\eta^* = 1 - \tfrac{4}{3}z + \tfrac{28}{9}z^2 + \cdots\,, \tag{3.15}$$

$$\Psi_1 = -2(1 - 2z + \tfrac{16}{3}z^2 + \cdots)\,. \tag{3.16}$$

We see that the USF for Maxwell molecules provides an example where the CE method converges.

For large shear rates, it is convenient to rewrite eq. (3.4) as

$$\lambda^* = \tfrac{1}{3}z^{1/3}[(9 + z^{-1} + 9\sqrt{1 + \tfrac{2}{9}z^{-1}})^{1/3} + (9 + z^{-1} - 9\sqrt{1 + \tfrac{2}{9}z^{-1}})^{1/3} - 2z^{-1/3}]\,. \tag{3.17}$$

This shows that, in order to expand about the point at infinity, the natural expansion variable is $z^{-1/3}$. The results are

$$\lambda^* = z^{1/3}[(\tfrac{2}{3})^{1/3} - \tfrac{2}{3}z^{-1/3} + \tfrac{1}{9}(\tfrac{3}{2})^{1/3}z^{-2/3} + \cdots]\,, \tag{3.18}$$

$$\eta^* = z^{-2/3}[(\tfrac{3}{2})^{2/3} - z^{-1/3} + \tfrac{1}{9}(\tfrac{3}{2})^{4/3}z^{-2/3} + \cdots]\,, \tag{3.19}$$

$$\Psi_1 = -z^{-1}[3 - 3(\tfrac{3}{2})^{1/3}z^{-1/3} + (\tfrac{3}{2})^{2/3}z^{-2/3} + \cdots]\,. \tag{3.20}$$

Most of the above results in this section can be found in ref. [12]. Let us turn our attention now to the VDF itself. With the definitions (2.13) and (2.14), eq.

(2.10) becomes

$$f^*(V^*, t) = \exp(-s) \exp[(t - t_0) a_{ij} V_j^* \, \partial/\partial V_i^*] \left(\frac{T}{T_0}\right)^{3/2} f^*\left(\sqrt{\frac{T}{T_0}}\, V^*, t_0\right)$$

$$+ \pi^{-3/2} \int_{t_0}^{t} \mathrm{d}t' \, \zeta(t') \exp[-(s - s')] \exp[(t - t') a_{ij} V_j^* \, \partial/\partial V_i^*]$$

$$\times \left(\frac{T}{T'}\right)^{3/2} \exp(-V^{*2} T/T') \,, \tag{3.21}$$

where $T \equiv T(t)$, $T' \equiv T(t')$ and $T_0 \equiv T(t_0)$. Eq. (3.21) provides the general solution and not just the normal one. To obtain the latter, we must take the limit $t - t_0 \to \infty$. In appendix A it is shown that, for any initial distribution,

$$\lim_{t - t_0 \to \infty} \left(\frac{T(t)}{T_0}\right)^{3/2} f^*\left(\sqrt{\frac{T(t)}{T_0}}\, V^*, t_0\right) = \delta(V^*) \,, \tag{3.22}$$

where $\delta(V^*)$ is Dirac's delta function. Both eqs. (3.21) and (3.22) are valid for any interaction potential. In the particular case of Maxwell molecules, the number of collisions s, defined by eq. (2.11), is just proportional to $t - t_0$. Thus, the first term in the right side of eq. (3.21) vanishes in the limit $t - t_0 \to \infty$. Concerning the second term, we can make, according to eq. (3.7),

$$\frac{T}{T'} = \exp[\lambda(t - t')] \,. \tag{3.23}$$

Although eq. (3.23) is not strictly true for times t' such that $t' - t_0$ is not large, the contribution to the integral coming from those times is negligible in the limit $t - t_0 \to \infty$ because of the factor $\exp[-(s - s')]$. After inserting eq. (3.23) into eq. (3.21), making the change of variable $s_1 = (t - t')\zeta$, and explicitly taking the limit $t - t_0 \to \infty$, we finally get

$$f^*(V^*; a^*) = \pi^{-3/2} \int_0^{\infty} \mathrm{d}s_1 \exp(-s_1) \exp(\tfrac{3}{2} \lambda^* s_1) \exp(a^* s_1 V_y^* \, \partial/\partial V_x^*)$$

$$\times \exp[-\exp(\lambda^* s_1) \, V^{*2}] \,. \tag{3.24}$$

Eq. (3.24) gives the explicit expression for the VDF representing the normal solution to the BGK equation for Maxwell molecules under USF. Notice that, although $f(V, t)$ depends on time, the reduced VDF f^* given by eq. (3.24) is constant in time for every value of the reduced velocity V. In this sense, the normal state for Maxwell molecules can be considered as equivalent to a steady

state [4]. The dependence on the reduced shear rate a^* appears explicitly and also through the function $\lambda^*(a^*)$ given by eq. (3.4). We see that the normal solution is analytic at $a^* = 0$. Consequently, the CE expansion of the VDF,

$$f^*(\boldsymbol{V}^*; a^*) = \sum_{k=0}^{\infty} a^{*k} f^{(k)}(\boldsymbol{V}^*) , \tag{3.25}$$

is convergent. This could be expected from the convergence of the expansions (3.14)–(3.16), but, in general, analyticity of the moments does not imply analyticity of the distribution function. The first few terms of the CE expansion of (3.24) can be easily obtained by making use of eq. (3.14):

$$\begin{aligned} f^*(\boldsymbol{V}^*; a^*) = \pi^{-3/2} \int_0^{\infty} ds_1 \exp(-s_1) [1 + a^{*2} s_1 + \mathcal{O}(a^{*4})] \\ \times \left(1 + a^* s_1 V_y^* \frac{\partial}{\partial V_x^*} + \tfrac{1}{2} a^{*2} s_1^2 V_y^{*2} \frac{\partial^2}{\partial V_x^{*2}} + \tfrac{1}{6} a^{*3} s_1^3 V_y^{*3} \frac{\partial^3}{\partial V_x^{*3}} + \mathcal{O}(a^{*4})\right) \\ \times [1 - \tfrac{2}{3} a^{*2} s_1 V^{*2} + \mathcal{O}(a^{*4})] \exp(-V^{*2}) . \end{aligned} \tag{3.26}$$

They are given by

$$f^{(0)}(\boldsymbol{V}^*) = \pi^{-3/2} \exp(-V^{*2}) , \tag{3.27}$$

$$f^{(1)}(\boldsymbol{V}^*) = -2 V_x^* V_y^* f^{(0)}(\boldsymbol{V}^*) , \tag{3.28}$$

$$f^{(2)}(\boldsymbol{V}^*) = [1 - \tfrac{2}{3} V^{*2} - 2 V_y^{*2} (1 - 2 V_x^{*2})] f^{(0)}(\boldsymbol{V}^*) , \tag{3.29}$$

$$f^{(3)}(\boldsymbol{V}^*) = 4 V_x^* V_y^* [V_y^{*2} (3 - 2 V_x^{*2}) + \tfrac{2}{3} V^{*2} - \tfrac{5}{3}] f^{(0)}(\boldsymbol{V}^*) . \tag{3.30}$$

As said before, the expansions (3.14)–(3.16) converge for $a^* < \sqrt{2}/3$. This is presumably also the radius of convergence of the expansion (3.25). For much larger values of the shear rate, the VDF diverges to infinity at $\boldsymbol{V} = \boldsymbol{0}$. This unexpected result happens when $\lambda^* \geq 2/3$, i.e. $a^* \geq 5/3$. In order to look at this point more closely, let us take $V_y^* = 0$. In that case, eq. (3.24) becomes

$$f^*(V_x^*, 0, V_z^*; a^*) = \frac{\pi^{-3/2}}{\lambda^*} V_\perp^{*\, 2(\lambda^{*-1} - 3/2)} \Gamma(\tfrac{3}{2} - \lambda^{*-1}, V_\perp^{*2}) , \tag{3.31}$$

where $V_\perp^{*2} \equiv V_x^{*2} + V_z^{*2}$ and

$$\Gamma(x, \varepsilon) \equiv \int_{\varepsilon}^{\infty} dt\, t^{x-1} \exp(-t) \tag{3.32}$$

is the incomplete gamma function [18]. It is well defined for all ε if $x>0$, and for $\varepsilon>0$ if $x\leq 0$. Its behavior in the limit $\varepsilon\to 0^+$ is obtained in appendix B (cf. eqs. (B.10)–(B.12)). Consequently,

$$f^*(V_x^*,0,V_z^*;a^*)\approx\begin{cases}\dfrac{\pi^{-3/2}}{1-\frac{3}{2}\lambda^*}, & \lambda^*<2/3, \quad (3.33a)\\ -\frac{3}{2}\pi^{-3/2}\ln V_\perp^{*2}, & \lambda^*=2/3, \quad (3.33b)\\ \pi^{-3/2}\lambda^{*-1}\Gamma(\frac{3}{2}-\lambda^{*-1})\,V_\perp^{*\,2(\lambda^{*-1}-3/2)}, & \lambda^*>2/3, \quad (3.33c)\end{cases}$$

in the limit $V_\perp^{*2}\to 0$. Eqs. (3.33b) and (3.33c) show that $f^*(\boldsymbol{V}^*;a^*)$ diverges when $\boldsymbol{V}^*\to\boldsymbol{0}$ if $\lambda^*\geq 2/3$. According to eq. (3.3), the corresponding range of shear rates is $a^*\geq 5/3$. The origin of this divergence at vanishing velocity is related to the viscous heating effect inherent to the USF. Two exponential terms compete in eq. (3.24). The first one, $\exp(-s_1)$, gives the fraction of particles that have not collided after s_1 collision times. The second term, $\exp(\frac{3}{2}\lambda^* s_1)$, is the ratio $[T(s_1)/T_0]^{3/2}$, which is a consequence of the nondimensionalizations (2.13) and (2.14). The first term goes to zero when $s_1\to\infty$, while the second one goes to infinity. For sufficiently small shear rates ($a^*<5/3$), the viscous heating is not enough to overcome the effect of collisions, so that the VDF is finite at $\boldsymbol{V}^*=\boldsymbol{0}$. However, the concentration of particles around $\boldsymbol{V}^*=\boldsymbol{0}$ is no longer counterbalanced by the collisions if $a^*\geq 5/3$, which results in the divergence of the VDF.

From eq. (3.24) it is a simple matter to obtain the functions defined in (2.19)–(2.21):

$$\tilde{f}^*(V_x^*,V_y^*;a^*)=\pi^{-1}\int_0^\infty ds_1\exp[-(1-\lambda^*)s_1]\exp(a^*s_1V_y^*\,\partial/\partial V_x^*)\times\exp[-\exp(\lambda^*s_1)(V_x^{*2}+V_y^{*2})], \quad (3.34)$$

$$F_x^{(+)}(V_x^*;a^*)=\frac{\pi^{-1/2}}{2}\int_0^\infty ds_1\,\frac{\exp[-(1-\frac{1}{2}\lambda^*)s_1]}{(1+a^{*2}s_1^2)^{1/2}}\exp\left(-\exp(\lambda^*s_1)\,\frac{V_x^{*2}}{1+a^{*2}s_1^2}\right)\times\operatorname{erfc}\left(\frac{a^*s_1}{(1+a^{*2}s_1^2)^{1/2}}\,V_x^*\exp(\tfrac{1}{2}\lambda^*s_1)\right), \quad (3.35)$$

$$F_y^{(+)}(V_y^*;a^*)=\frac{\pi^{-1/2}}{2}\int_0^\infty ds_1\exp[-(1-\tfrac{1}{2}\lambda^*)s_1]\exp[-\exp(\lambda^*s_1)\,V_y^{*2}]\times\operatorname{erfc}[a^*s_1V_y^*\exp(\tfrac{1}{2}\lambda^*s_1)], \quad (3.36)$$

where erfc(x) is the complementary error function [18]. The functions $\tilde{f}^*$ and $F_{x,y}^{(+)}$ now diverge at the velocity origin for $a^* \geq \sqrt{6}$ and $a^* \geq 3\sqrt{3}$, respectively.

Fig. 1 shows the ratio

$$\tilde{\varphi}(V_x^*, V_y^*; a^*) = \frac{\tilde{f}^*(V_x^*, V_y^*; a^*)}{\tilde{f}^{(0)}(V_x^*, V_y^*)}, \tag{3.37}$$

for $a^* = 1$ and $-2 \leq V_{x,y}^* \leq 2$, where

$$\tilde{f}^{(0)}(V_x^*, V_y^*) = \pi^{-1} \exp[-(V_x^{*2} + V_y^{*2})] \tag{3.38}$$

is the local equilibrium function. The distortion from local equilibrium at this rather large shear rate is quite apparent. In fact, the value $a^* = 1$ is beyond the convergence region ($a^* \leq \sqrt{2}/3$) of the CE expansion (3.25).

A much larger distortion occurs when a^* exceeds the threshold value $a^* = \sqrt{6}$. As an example, the case $a^* = 4$ is considered in fig. 2. The qualitative shape is very different from that of fig. 1. However, the divergence at $V_x^* = V_y^* = 0$ does not show up in fig. 2. This is because the trend to that divergence is only apparent for values of V_x^* and V_y^* much smaller than the grid size chosen in fig. 2. The region $-0.005 \leq V_{x,y}^* \leq 0.005$ is amplified in fig. 3, where now the expected behavior of $\tilde{\varphi}$ in the neighborhood of the origin is clearly observed.

The knowledge of the VDF allows one to get explicit expressions for the velocity moments

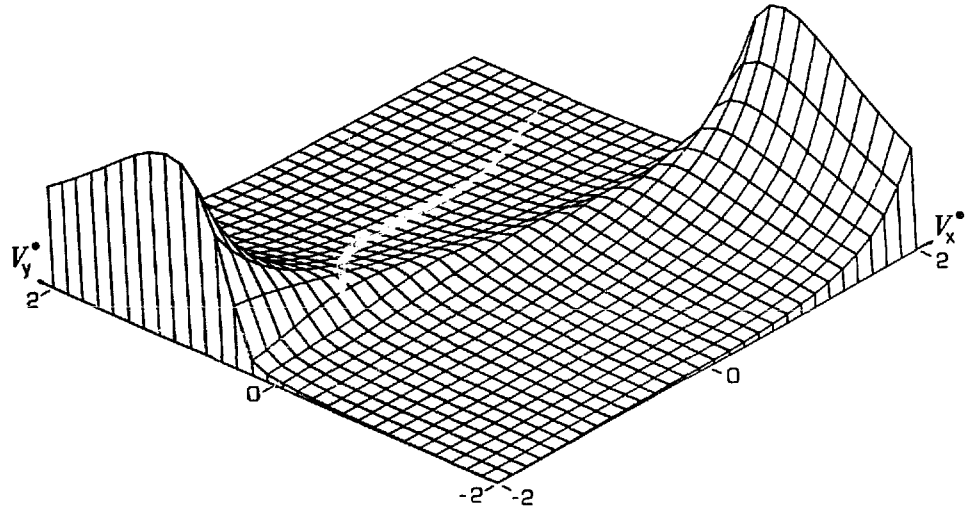

Fig. 1. Surface plot of the VDF relative to local equilibrium, $\tilde{\varphi}(V_x^*, V_y^*; a^*)$, in the case of Maxwell molecules for a reduced shear rate $a^* = 1$. Maximum value is 10.5.

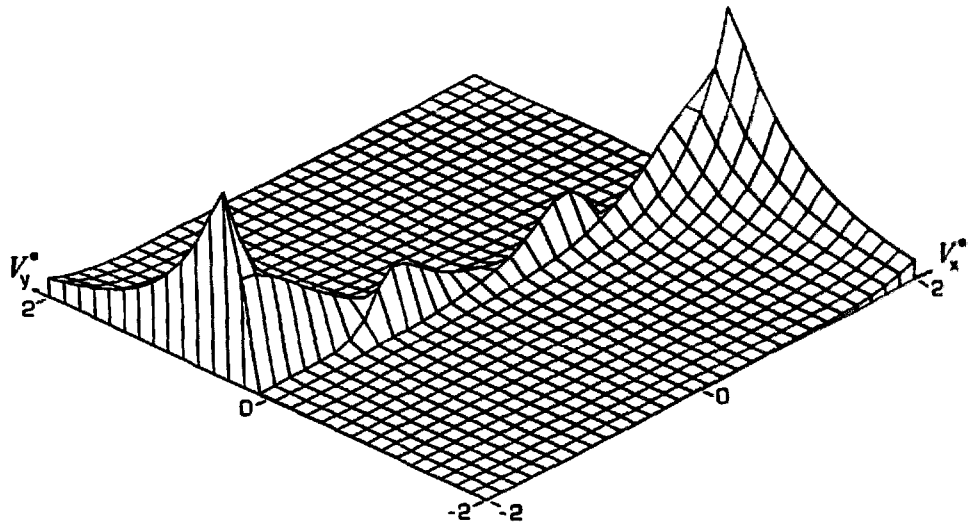

Fig. 2. Same as fig. 1, but for $a^* = 4$. Maximum value is 21.6.

$$M_{k_1,k_2,k_3}(a^*) = \int \mathrm{d}\boldsymbol{V}^*\, V_x^{*k_1} V_y^{*k_2} V_z^{*k_3} f^*(\boldsymbol{V}^*; a^*)\,. \tag{3.39}$$

The only nonvanishing moments correspond to $k_1 + k_2$ and k_3 even. In that case, substituting eq. (3.24) into eq. (3.39), one has

$$M_{k_1,k_2,k_3}(a^*) = \pi^{-3/2} \int_0^\infty \mathrm{d}s_1 \exp[-(1 - \tfrac{3}{2}\lambda^*)s_1] \int \mathrm{d}\boldsymbol{V}^* \exp[-\exp(\lambda^* s_1)\, V^{*2}] \times (V_x^* - a^* s_1 V_y^*)^{k_1} V_y^{*k_2} V_z^{*k_3}$$

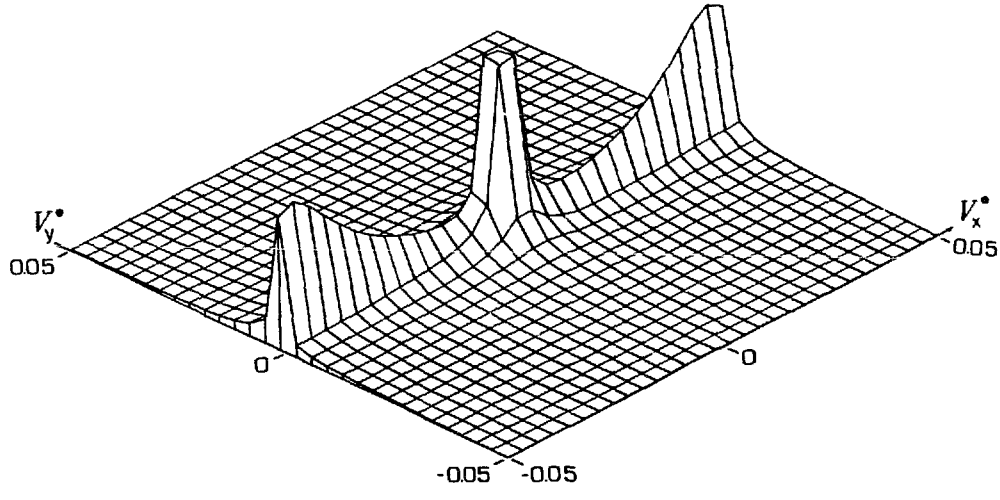

Fig. 3. Same as fig. 2, but for a much smaller region of velocities. Maximum value is 118.

$$= \pi^{-3/2} \sum_{\substack{q=0 \\ q+k_1=\text{even}}}^{k_1} \binom{k_1}{q} \Gamma\left(\frac{k_1-q+1}{2}\right) \Gamma\left(\frac{k_2+q+1}{2}\right) \Gamma\left(\frac{k_3+1}{2}\right)$$

$$\times \int_0^\infty ds_1 \, (-a^* s_1)^q \exp\left[-\left(1+\frac{k_1+k_2+k_3}{2}\lambda^*\right)s_1\right]. \tag{3.40}$$

After performing the s_1-integration, we finally get

$$M_{k_1,k_2,k_3}(a^*)$$

$$= \pi^{-3/2} \sum_{\substack{q=0 \\ q+k_1=\text{even}}}^{k_1} \frac{k_1!}{(k_1-q)!} \Gamma\left(\frac{k_1-q+1}{2}\right) \Gamma\left(\frac{k_2+q+1}{2}\right) \Gamma\left(\frac{k_3+1}{2}\right)$$

$$\times (-a^*)^q \left(1+\frac{k_1+k_2+k_3}{2}\lambda^*\right)^{-(1+q)}. \tag{3.41}$$

In particular, eqs. (2.16), (2.18), (3.8) and (3.9) are recovered.

Once we have analyzed in some detail the VDF given by eq. (3.24), it is instructive to obtain the rate of change of the entropy density

$$S(t) = -k_B \int d\boldsymbol{V} \, f(\boldsymbol{V}, t) \ln f(\boldsymbol{V}, t) \tag{3.42}$$

after the hydrodynamic stage is reached [19]. Rather than the detailed structure of eq. (3.24), which is crucial is the fact that, for a given value of the reduced velocity $\boldsymbol{V}^*$, the reduced VDF f^* does not change in time, since a^* is a constant. This is not true for interactions other than Maxwell's [19]. Use of the changes (2.13) and (2.14) gives

$$S(t) = -nk_B \int d\boldsymbol{V}^* \, f^*(\boldsymbol{V}^*; a^*) \ln\left[n\left(\frac{m}{2k_B T(t)}\right)^{3/2} f^*(\boldsymbol{V}^*; a^*)\right], \tag{3.43}$$

and, therefore,

$$\frac{dS(t)}{dt} = \tfrac{3}{2} n k_B \frac{1}{T(t)} \frac{dT(t)}{dt}. \tag{3.44}$$

Comparison of this equation with the thermodynamics fundamental equation (for an ideal gas)

$$dS = \tfrac{3}{2} n k_B \frac{dT}{T} - \frac{p}{T} \frac{dn}{n}, \tag{3.45}$$

shows that local equilibrium thermodynamics holds for a gas of Maxwell molecules under USF arbitrarily far from equilibrium. Eqs. (3.7) and (3.44) also show that $S(t)$ grows linearly in time.

4. Power-law repulsive potentials. Hard spheres

In this section, we are going to consider interaction potentials of the form $V(r) - r^{-l}$, for which the collision frequency is given by eq. (1.9). Since the particular case of Maxwell molecules ($\alpha = 0$) has already been analyzed in the previous section, we shall consider now the case $\alpha > 0$, with special attention to $\alpha = 1/2$ (hard spheres). Eventually, the limit $\alpha \to 0^+$ will be taken to recover some of the results of section 3.

For Maxwell molecules the reduced shear rate $a^* = a/\zeta$ is a constant, so that the system is always the same distance apart from equilibrium. It was then natural to expect the system to reach a hydrodynamic regime after a certain transient period. Nevertheless, a^* decreases in time in the more general case of $\alpha > 0$. Thus, as time grows, the state of the system is closer and closer to that of (local) equilibrium. Consequently, the existence of a normal solution beyond states asymptotically close to equilibrium is not evident. As we shall see, a far from equilibrium normal solution exists in the limit of infinite times but finite collision times.

Let us start by analyzing the nonlinear set of equations (2.7)–(2.9), with $\zeta \propto p^\alpha$. Elimination of t in favor of $z \equiv a^{*2}$ yields, after some algebra,

$$\tfrac{8}{9}\alpha^2 z^4 \eta^* \frac{\partial^2}{\partial z^2}\eta^{*2} - \tfrac{4}{3}\alpha z^2[1 + 2z(\tfrac{1}{2} - \alpha)\eta^*]\frac{\partial}{\partial z}\eta^{*2} + \eta^*[1 + \tfrac{2}{3}(2-\alpha)z\eta^* + \tfrac{8}{9}(\tfrac{1}{2} - \alpha)(1-\alpha)z^2\eta^{*2}] = 1 , \tag{4.1}$$

where we recall that $\eta^* \equiv -(P_{xy}/p)/a^*$ is the reduced shear viscosity. The evolution equation for a^* is

$$\frac{1}{a}\frac{\partial a^*}{\partial t} = -\tfrac{2}{3}\alpha a^{*2}\eta^{*2} . \tag{4.2}$$

Given an initial VDF $f(V, t_0)$, one gets the initial values of the shear rate (a_0^*), the shear viscosity (η_0^*), and the derivative $\eta_0^{*\prime} = (\partial\eta^*/\partial z)_{t=t_0}$. The latter is given by

$$\eta_0^{*\prime} = \frac{3}{4\alpha} a_0^{*-4}\left[1 - a_0^*\left(\tfrac{2}{3}(1-\alpha)P_{xy}^*(t_0) - \frac{P_{yy}^*(t_0)}{P_{xy}^*(t_0)}\right)\right] . \tag{4.3}$$

With the above initial conditions, eq. (4.1) provides $\eta^*(a^*)$ for $a^* < a_0^*$. In principle, there are as many particular solutions as initial conditions. As an example, let us take the following two-parameter family of initial VDFs:

$$f(\mathbf{V}, t_0) = n\left(\frac{\beta}{\pi}\right)^{3/2} \exp(\varepsilon V_y \partial/\partial V_x) \exp(-\beta V^2) . \tag{4.4}$$

This function is an anisotropic Gaussian. The parameter ε is a measure of the coupling between V_x and V_y, while β is related to the initial temperature T_0 or, equivalently, to the initial shear rate a_0^*. Fig. 4 shows the numerical solutions of eq. (4.1) in the case of hard spheres ($\alpha = 1/2$) for the initial condition (4.4) with $\varepsilon = 0.01$ and 1, and $a_0^* = 1$ and $\sqrt{2}$. It is seen that the four particular solutions tend to overlap for values of a^* sufficiently smaller than the initial one. A similar behavior can be observed when starting from other initial conditions. Thus, there must exist a special solution of eq. (4.1) that "attracts" all the particular solutions. It seems then logical to identify that special solution with the generalized hydrodynamic viscosity $\eta^*(a^*)$.

In order to get a useful representation for the hydrodynamic viscosity, one could try a (CE) power expansion,

$$\eta^*(a^*) = 1 + \sum_{k=1}^{\infty} c_k z^k . \tag{4.5}$$

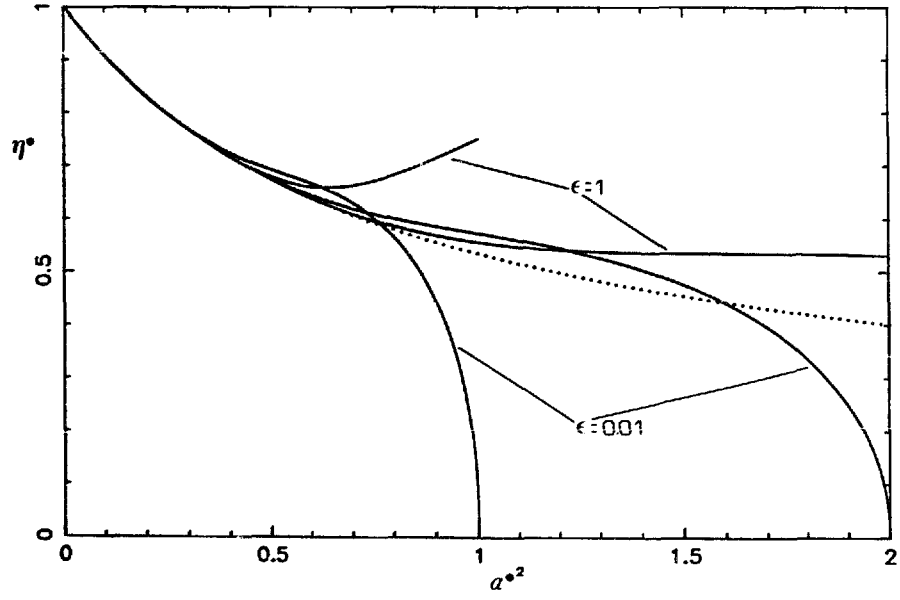

Fig. 4. Particular solutions of eq. (4.1) for hard spheres ($\alpha = 1/2$) corresponding to 4 initial conditions of the form given by eq. (4.4). The dotted line corresponds to the special solution represented by the series (4.10).

In the case of Maxwell molecules, this expansion, given by eq. (3.15), is convergent. Substituting eq. (4.5) into eq. (4.1) for $\alpha > 0$, one can obtain the coefficients c_k recursively (see appendix C). The first few ones are

$$c_1 = -\tfrac{2}{3}(2-\alpha)\,, \tag{4.6a}$$

$$c_2 = \tfrac{4}{9}(7-13\alpha+4\alpha^2)\,, \tag{4.6b}$$

$$c_3 = \tfrac{8}{9}(-10-39\alpha-39\alpha^2+9\alpha^3)\,. \tag{4.6c}$$

A dominant-term analysis carried out in appendix C shows the consistency of the behavior

$$|c_k| \sim k!(\tfrac{4}{3}\alpha)^k \tag{4.7}$$

for large k. Therefore, the series (4.5) is only asymptotic. The divergence of the series (4.5) and the asymptotic behavior (4.7) have been numerically confirmed in the case of hard spheres [20]. Thus, the series (4.5) holds for any solution of eq. (4.1) and does not characterize a particular solution, not even the hydrodynamic one.

The generalized hydrodynamic viscosity can be obtained by means of a power expansion around the point at infinity. An analysis of eq. (4.1) for large z indicates that either

$$\eta^* \approx \mathscr{A} z^{(1-\alpha)/2\alpha} \tag{4.8}$$

with $\mathscr{A}$ arbitrary, or

$$\eta^* \approx \bar{c}_0 z^{-2/3}\,, \qquad \bar{c}_0 = [\tfrac{8}{9}(\tfrac{1}{3}\alpha+1)(\tfrac{1}{3}\alpha+\tfrac{1}{2})]^{-1/3}\,. \tag{4.9}$$

The first asymptotic behavior, eq. (4.8), corresponds to the general solution of eq. (4.1). The second behavior, eq. (4.9), is universal (in the sense that the power of z is independent of the value of α) and defines a special solution of eq. (4.1). Such a special solution can be represented by the expansion

$$\eta^*(a^*) = z^{-2/3} \sum_{k=0}^{\infty} \bar{c}_k (z^{-1/3})^k\,, \tag{4.10}$$

which has the same form as in the case of Maxwell molecules, eq. (3.19). The first three coefficients are $\bar{c}_0$, given in eq. (4.9), and

$$\bar{c}_1 = -\frac{1}{2}\,\frac{6+5\alpha}{3+5\alpha+2\alpha^2}\,, \tag{4.11a}$$

$$\bar{c}_2 = -\frac{9+4(6+7\alpha)\bar{c}_1+4(3+7\alpha-\frac{34}{9}\alpha^2)\bar{c}_1^2}{4(3+7\alpha+\frac{38}{9}\alpha^2)\bar{c}_0}\,. \tag{4.11b}$$

In contrast to the series (4.5), the series (4.10) is convergent. In the case of hard spheres, for instance, $|\bar{c}_k| \sim (3^{-2/3})^k$ and the series (4.10) converges for $a^* > 1/3$ [20]. The dotted line in fig. 4 corresponds to the hydrodynamic viscosity for hard spheres as obtained from the series (4.10). The same function is plotted in fig. 5 for a wider range of shear rates. For comparison, the viscosity for Maxwell molecules, eq. (3.11), is also shown. It is seen that the general shape of the reduced shear viscosity is rather insensitive to the details of the interaction potential. This is somewhat unexpected if one takes into account the fact that both functions differ in an important qualitative feature, namely the convergent character of the series expansion around the origin, eq. (4.5).

Regarding the other components of the pressure tensor, eq. (2.6) yields, in reduced units,

$$\left(\tfrac{2}{3}\alpha a^{*2}P^*_{xy}\frac{\partial}{\partial a^*}+1\right)P^*_{ij}+a^*_{ik}P^*_{kj}+a^*_{jk}P^*_{ki}-\tfrac{2}{3}a^*P^*_{xy}P^*_{ij}=\delta_{ij}\,. \tag{4.12}$$

In a normal state, we have

$$P^*_{xz}=P^*_{yz}=0\,, \tag{4.13}$$

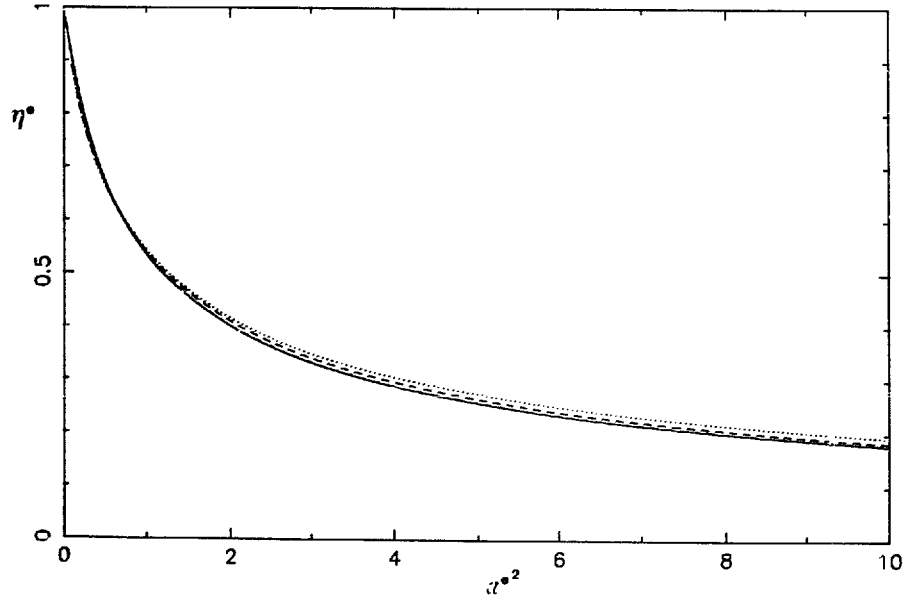

Fig. 5. Plot of the (hydrodynamic) shear viscosity for Maxwell molecules (dotted line), hard spheres (solid line), and an approximation of the latter, given by eq. (4.35) (dashed line).

$$P_{yy}^* P_{zz}^* = \tfrac{2}{3} P_{xy}^{*2} - \frac{P_{xy}^*}{a^*} - \tfrac{2}{3}\alpha a^* P_{xy}^* \frac{\partial P_{xy}^*}{\partial a^*} . \tag{4.14}$$

Consequently, the viscometric functions are

$$\Psi_1(a^*) = 3\frac{\eta^* - 1}{z} + 2(1-\alpha)\eta^{*2} - 2\alpha z \frac{\partial \eta^{*2}}{\partial z} , \tag{4.15}$$

$$\Psi_2(a^*) = 0 . \tag{4.16}$$

The expansions (4.5) and (4.10) give, respectively,

$$\Psi_1(a^*) = -2[1 - 2(1-\alpha)z + 8(\tfrac{1}{2} - \alpha)(\tfrac{4}{3} - \alpha)z^2 + \cdots] , \tag{4.17}$$

$$\Psi_1(a^*) = -z^{-1}[3 - 2(1 + \tfrac{1}{3}\alpha)\bar{c}_0^2 z^{-1/3} + \cdots] . \tag{4.18}$$

Let us discuss now the idea underlying in the method used to take the hydrodynamic limit of long times and get the representation (4.10) for the shear viscosity. If one fixes an initial condition at a given time t_0 (which corresponds to a certain a_0^*) and then takes the limit $t - t_0 \to \infty$, it is clear that the result is $a^* = 0$. This strategy is inadequate, since it reduces the normal solution to states asymptotically close to equilibrium. Rather than fixing the present at t_0 and to look towards an infinitely far future ($t \to \infty$), it is more useful to fix the present at t and push away the initial condition to the remote past ($t_0 \to -\infty$). According to the second point of view, we fix a value of a^* and obtain the normal solution corresponding to it by formally applying the initial condition for $a_0^* \to \infty$ or, equivalently, $T_0 \to 0$. An important consequence is that, except in the case of Maxwell molecules, the effective number of collisions taking place between t_0 and t, given by eq. (2.11), is kept finite as $t_0 \to -\infty$:

$$\lim_{t_0 \to -\infty} s(t) = \frac{3}{2\alpha} \int_{a'}^{\infty} \mathrm{d}a^{*\prime} \, [a^{*\prime 3} \eta^*(a^{*\prime})]^{-1} , \tag{4.19}$$

where use has been made of eq. (4.2). From eq. (4.9) we see that $a^{*3}\eta^*(a^*) \sim a^{*5/3}$ for large a^*, so that the integral in eq. (4.19) is finite. Consequently, the VDF, eq. (3.21) possesses a contribution associated to the initial condition term. This contribution, however, becomes independent of the details of the initial distribution in the long-time limit, as shown by eq. (3.22). Therefore, the normal solution to the BGK equation reads

$$f^*(V^*;a^*)=\exp(-\sigma/\alpha)\,\delta(V^*)+\frac{\pi^{-3/2}}{\alpha}\int_0^{\sigma}d\sigma'\exp[-(\sigma-\sigma')/\alpha]\left(\frac{a^{*\prime}}{a^*}\right)^{3/2\alpha}\times\exp\left(\frac{\tau-\tau'}{\alpha}V_y^*\partial/\partial V_x^*\right)\exp\left[-\left(\frac{a^{*\prime}}{a^*}\right)^{1/\alpha}V^{*2}\right],\tag{4.20}$$

where $\sigma\equiv\alpha s$, $\tau\equiv\alpha a t$, $a^{*\prime}\equiv a^*(\sigma')$, and $\tau'\equiv\tau(\sigma')$. The variables a^*, τ and σ are related each other by the differential equations

$$\frac{\partial a^*}{\partial\sigma}=-\tfrac{2}{3}a^{*3}\eta^*(a^*)\,,\tag{4.21}$$

$$\frac{\partial\tau}{\partial\sigma}=a^*\,.\tag{4.22}$$

Eqs. (4.21) and (4.22) follow directly from eqs. (2.11) and (4.2). The solution of eq. (4.21), where $\eta^*(a^*)$ is given by the series (4.10), with the boundary condition $a^*\to\infty$ when $\sigma\to 0$, gives σ as a function of a^* or, equivalently, a^* as a function of σ. Inserting the latter into eq. (4.22) and applying the boundary condition $\tau\to-\infty$ when $\sigma\to 0$, one gets τ as a function of σ or, analogously, as a function of a^*. Substitution of all these functions into eq. (4.20) provides the normal VDF $f^*(V^*;a^*)$ for any desired value of the reduced shear rate a^*. All of this can be achieved numerically very easily.

The choice of the variables σ and τ instead of s and t, respectively, is suggested by the convenience of making the dependence on the potential parameter α in eq. (4.20) as explicit as possible. Of course, the functions $\sigma(a^*)$ and $\tau(a^*)$ depend on the value of α, since so does the shear viscosity $\eta^*(a^*)$. Nevertheless, given the weak influence of α on $\eta^*(a^*)$ observed in fig. 5, one can also expect a small influence on $\sigma(a^*)$ and $\tau(a^*)$. This is confirmed by fig. 6, where a^{*-2} is plotted versus σ for hard spheres ($\alpha=1/2$) and for Maxwell molecules ($\alpha=0$). The first curve is obtained from the numerical solution of eq. (4.21), while the second one can be obtained analytically (see appendix D):

$$\sigma_{\rm M}(a^*)=\tfrac{1}{2}\lambda^{*-1}+\ln(1+\lambda^{*-1})\,,\tag{4.23}$$

where the subindex M is used here to emphasize that eq. (4.23) corresponds to the singular limit of Maxwell molecules ($\alpha\to 0$). In fact, the function $\sigma(a^*)$ does not have any special meaning in the context of Maxwell molecules. Let us remind that $s(a^*)$ represents the total effective number of collisions per particle needed to reach a shear rate a^* when starting from a much larger value a_0^* (formally, $a_0^*\to\infty$). Such a number of collisions strongly depends on the interaction potential through the parameter α. The "quasi-universal" behavior

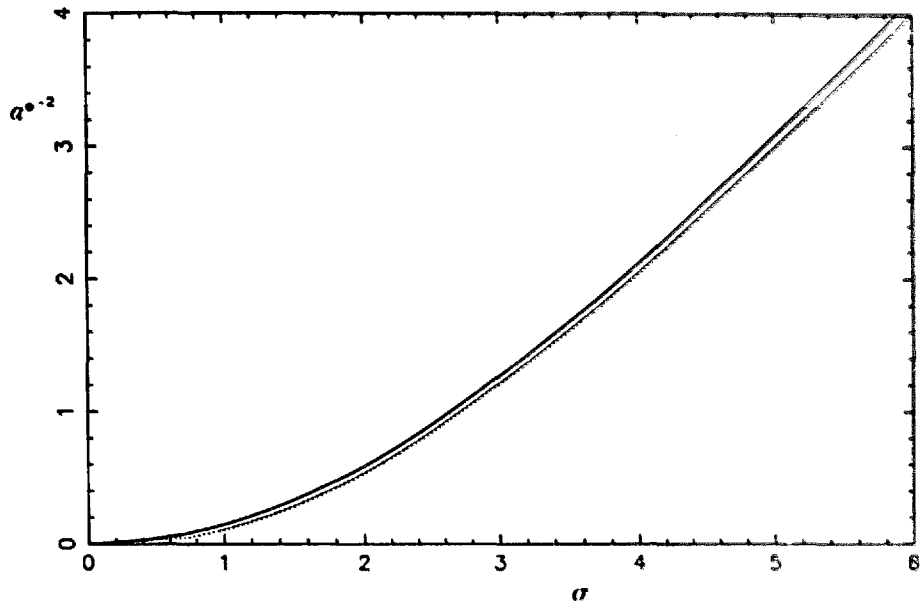

Fig. 6. Plot of a^{*-2} versus σ for hard spheres (solid line) and Maxwell molecules (dotted line).

of $\sigma(a^*)$ indicates that, roughly speaking, $s \propto \alpha^{-1}$. Since $a^{*-2} \propto T^{2\alpha}$, the curve for hard spheres in fig. 6 can also be understood as a plot of T versus s. The slope of this curve gives directly the shear viscosity, according to eq. (4.21). This was essentially the method used by Naitoh and Ono [21] to measure the shear viscosity from molecular dynamics data.

The main qualitative difference between the VDF for Maxwell molecules, eq. (3.24), and the one for more general potentials, eq. (4.20), is the presence in the latter of the delta term. It represents the contribution to the VDF of the fraction of particles that have not collided yet after a period of time equivalent to $s = \sigma/\alpha$ collisions. In a strict sense, all those particles have still the same velocities as initially. However, due to viscous heating, those velocities are negligibly small as compared to the thermal velocity at the time under consideration. From this point of view, the VDF (4.20) is independent of the initial conditions and hence can be considered as normal. If the stronger criterion of an infinite number of collision times were imposed, then the normal VDF would reduce to that of local equilibrium.

The presence of the delta term is reminiscent of the divergence of the VDF for Maxwell molecules, given by eq. (3.24), in the limit $V^* \to 0$. In contrast to the latter, however, the divergence exists now for any value of a^*. The first terms in the CE expansion (3.25) are still given by eqs. (3.27)–(3.29), even if $\alpha \neq 0$ [19], and are regular at $V^* = 0$. Consequently, the CE expansion of eq. (4.20) is only asymptotic.

As a check of consistency, it is straightforward to verify that eq. (4.20) identically satisfies the conditions (2.16) and (2.17) with independence of the form of the functions $\sigma(a^*)$ and $\tau(a^*)$. On the other hand, eq. (2.18) implies

$$\frac{1}{\alpha}\int_0^{\sigma} d\sigma'\left[1+\frac{1}{3}\left(\frac{\tau-\tau'}{\alpha}\right)^2\right]\exp\left[-\frac{1}{\alpha}\left(\sigma-\sigma'+\ln\frac{a^{*\prime}}{a^*}\right)\right]=1\,. \tag{4.24}$$

This is an implicit equation for $\eta^*(a^*)$. By differentiating with respect to σ, one has

$$\eta^*(a^*)=\frac{1}{\alpha^2}\frac{1}{a^*}\int_0^{\sigma} d\sigma'\,(\tau-\tau')\exp\left[-\frac{1}{\alpha}\left(\sigma-\sigma'+\ln\frac{a^{*\prime}}{a^*}\right)\right]. \tag{4.25}$$

The above equation can also be obtained by multiplying both sides of eq. (4.20) by $V_x^* V_y^*$ and integrating over $\boldsymbol{V}^*$. Eq. (4.25), along with eqs. (4.21) and (4.22), provides the special solution of eq. (4.1) compatible with the boundary condition (4.9), in a representation different from that of eq. (4.10).

Fig. 7 shows the regular part of the ratio (3.37) for $a^* = 4$ in the case of hard spheres ($\alpha = 1/2$). The general appearance is not very different from that of fig. 2. However, the magnification of the small velocity region, fig. 8, does not have any resemblance with fig. 3. The continuous, although very sharp, increasing of the distribution near $\boldsymbol{V} = \boldsymbol{0}$ for $\alpha = 0$ is replaced by a delta-peak, not shown in fig. 8, in the case of $\alpha \neq 0$.

In order to compare more closely the distribution functions corresponding to Maxwell molecules and hard spheres, it is convenient to consider the one-variable functions (2.20) and (2.21). In the case of Maxwell molecules, those functions are given by eqs. (3.35) and (3.36). On the other hand, for $\alpha \neq 0$, eq. (4.20) yields

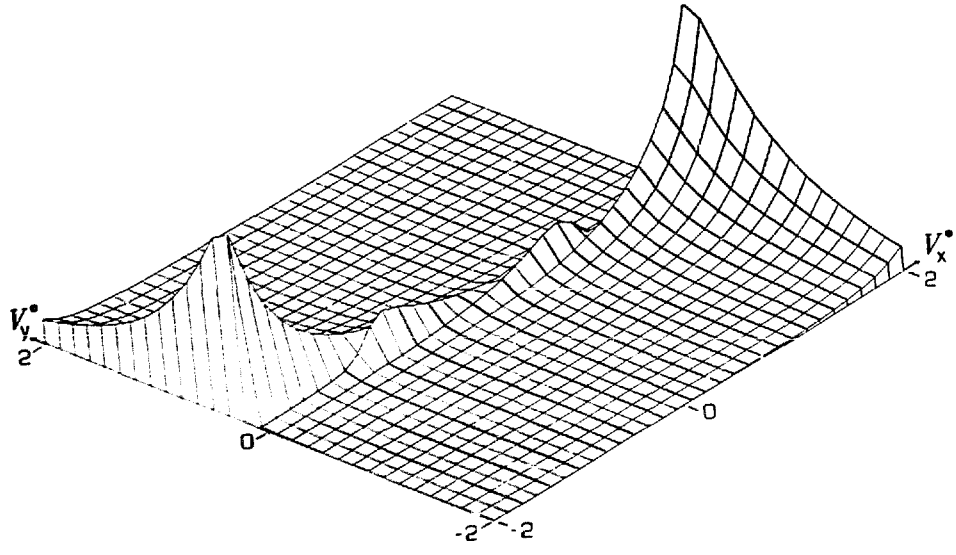

Fig. 7. Surface plot of the VDF relative to local equilibrium, $\tilde{\varphi}(V_x^*, V_y^*; a^*)$, in the case of hard spheres for a reduced shear rate $a^* = 4$. Maximum value is 17.3.

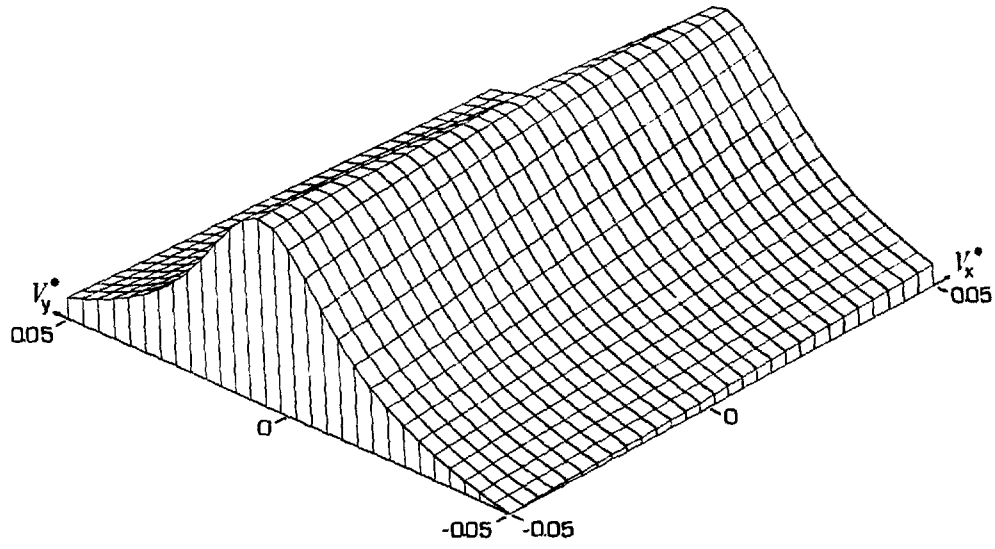

Fig. 8. Same as fig. 7, but for a much smaller region of velocities. Minimum and maximum values are 1.3 and 3.8, respectively.

$$F_x^{(+)}(V_x^*;a^*)=\frac{1}{2}\,\frac{\pi^{-3/2}}{\alpha}\int_0^\sigma d\sigma'\exp[-(\sigma-\sigma')/\alpha]\left(\frac{a^{*\prime}}{a^*}\right)^{1/2\alpha}$$
$$\times\left[1+\left(\frac{\tau-\tau'}{\alpha}\right)^2\right]^{-1/2}\exp\left\{-\left(\frac{a^{*\prime}}{a^*}\right)^{1/\alpha}\left[1+\left(\frac{\tau-\tau'}{\alpha}\right)^2\right]^{-1}V_x^{*2}\right\}$$
$$\times\operatorname{erfc}\left[\left(\frac{a^{*\prime}}{a^*}\right)^{1/2\alpha}\frac{(\tau-\tau')/\alpha}{\{1+[(\tau-\tau')/\alpha]^2\}^{1/2}}V_x^*\right], \tag{4.26}$$

$$F_y^{(+)}(V_y^*;a^*)=\frac{1}{2}\,\frac{\pi^{-3/2}}{\alpha}\int_0^\sigma d\sigma'\exp[-(\sigma-\sigma')/\alpha]\left(\frac{a^{*\prime}}{a^*}\right)^{1/2\alpha}$$
$$\times\exp[-(a^{*\prime}/a^*)^{1/\alpha}V_y^{*2}]\operatorname{erfc}\left[\left(\frac{a^{*\prime}}{a^*}\right)^{1/2\alpha}\frac{\tau-\tau'}{\alpha}V_y^*\right], \tag{4.27}$$

where only the regular part of the VDF has been considered. The ratios

$$\Phi_x^{(+)}(V_x^*;a^*)=\frac{F_x^{(+)}(V_x^*;a^*)}{F^{(0)}(V_x^*)}, \tag{4.28}$$

$$\Phi_y^{(+)}(V_y^*;a^*)=\frac{F_y^{(+)}(V_y^*;a^*)}{F^{(0)}(V_y^*)}, \tag{4.29}$$

where $F^{(0)}$ is the corresponding local equilibrium function, are shown in figs. 9 and 10 for $a^*=1$. For this not too large shear rate, the distributions for

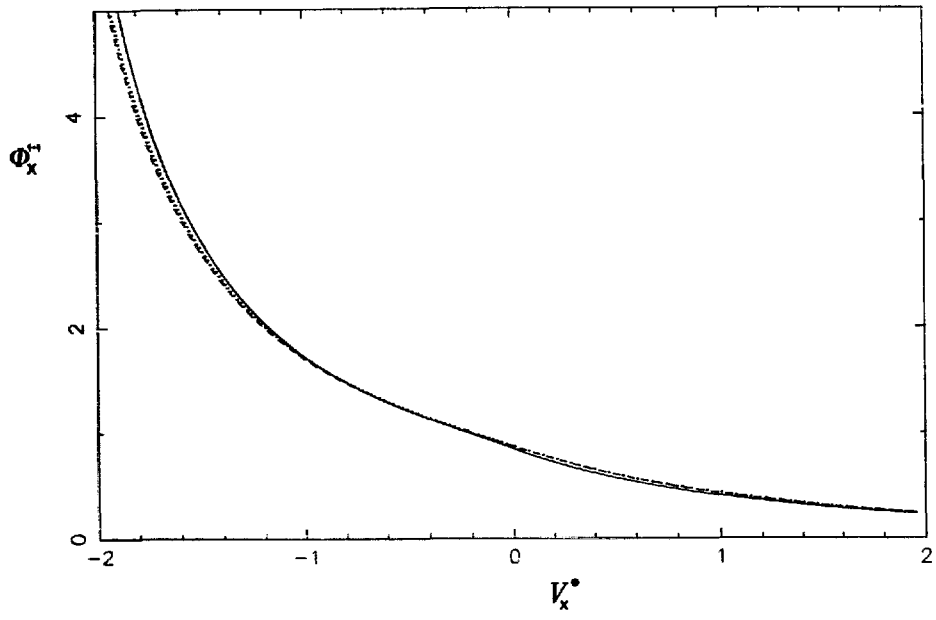

Fig. 9. The VDF relative to local equilibrium, $\Phi_x^{(+)}(V_x^*; a^*)$, versus V_x^* for $a^* = 1$. The dotted line corresponds to Maxwell molecules, the solid line corresponds to hard spheres, and the dashed line refers to an approximation of the latter, eq. (4.34).

Maxwell molecules and for hard spheres agree rather well. Since $a^* = 1$ is smaller than the threshold value $a^* = 3\sqrt{3}$, the functions for Maxwell molecules remain finite in the vicinity of $V_x^* = 0$ and $V_y^* = 0$. Regarding the case of hard spheres, the practical importance of the delta term is very small, since $s = 5.28$ for $a^* = 1$. Figs. 11 and 12 show the same as figs. 9 and 10, but for

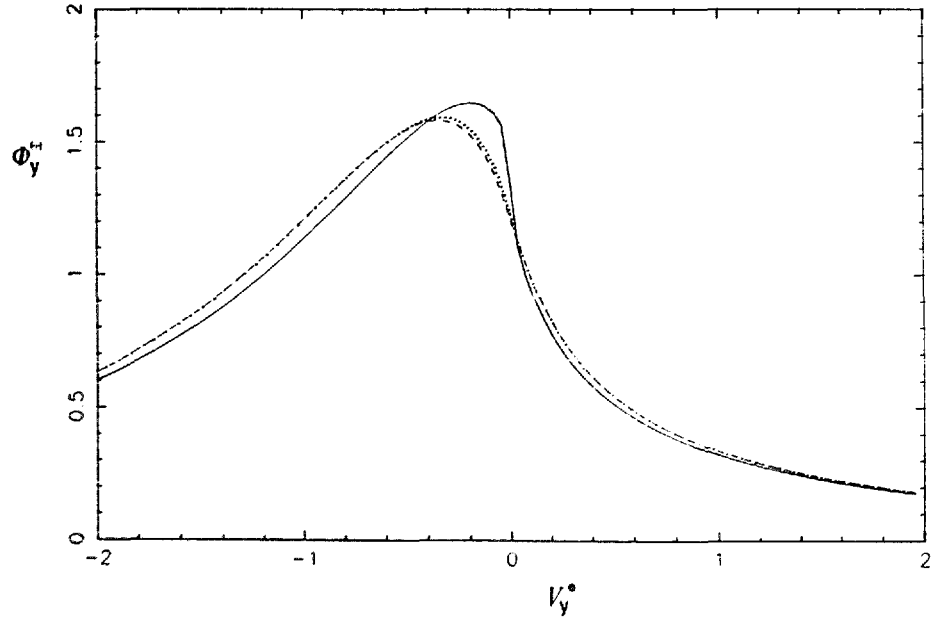

Fig. 10. Same as fig. 9, but for $\Phi_y^{(+)}(V_y^*; a^*)$ as a function of V_y^*.

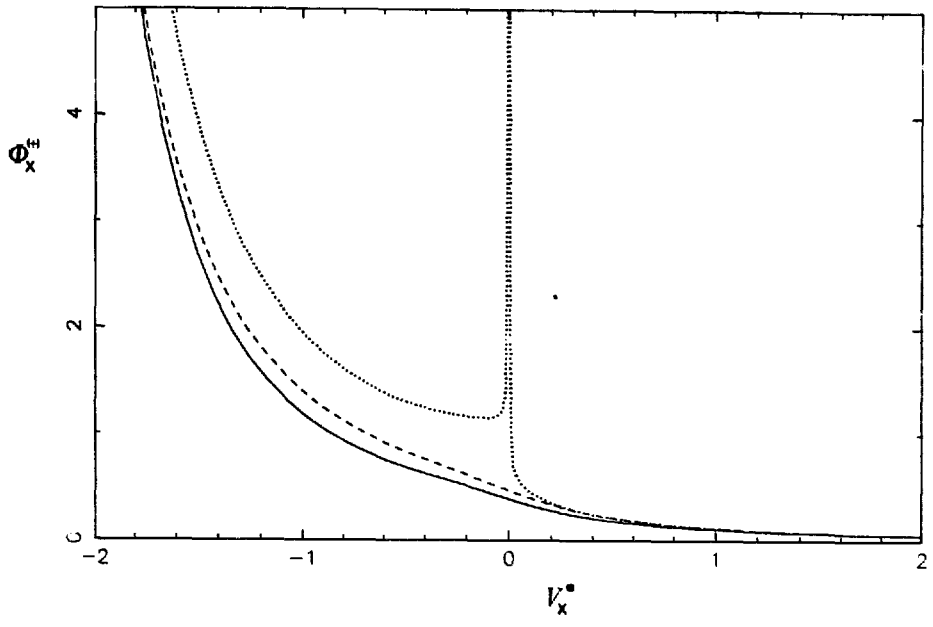

Fig. 11. Same as fig. 9, but for $a^* = 6$.

$a^* = 6$. The qualitative differences between Maxwell molecules and hard spheres are now quite evident. In the latter case, the number of collisions is $s = 0.80$, so that 45% of the particles have zero velocity.

Despite the feasibility of the numerical evaluation of eq. (4.20), its intricate dependence on a^* makes difficult the analysis of such features as the nature of the singularity at $a^* = 0$ and its disappearance in the limit of Maxwell molecules ($\alpha \to 0$). For that reason, it is useful to construct an approximate VDF

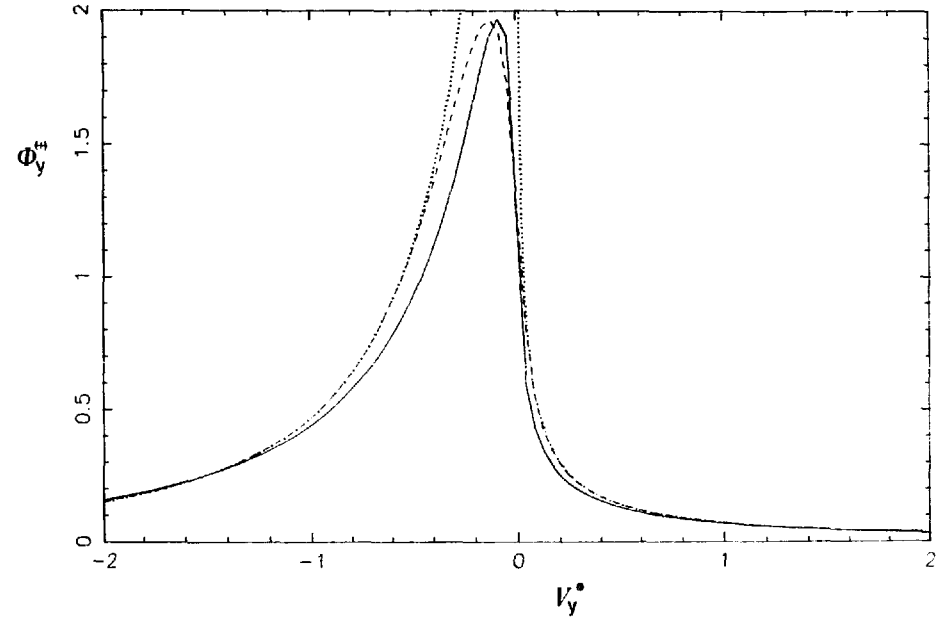

Fig. 12. Same as fig. 10, but for $a^* = 6$.

starting from eq. (4.20) and trying to keep the most relevant features of the actual VDF. This approximate model will be obtained following two steps. In the first step, we notice that the integrand in eq. (4.20) has a very sharp maximum at $\sigma = \sigma'$ in the limit $\alpha \to 0^+$. In that case, eqs. (4.21) and (4.22) yield, near the maximum,

$$\ln \frac{a^{*\prime}}{a^*} \simeq \tfrac{2}{3} a^{*2} \eta^*(a^*)\,(\sigma - \sigma')\,, \tag{4.30}$$

$$\tau - \tau' \simeq a^*(\sigma - \sigma')\,. \tag{4.31}$$

Consequently, eq. (4.20) becomes

$$f^*(V^*; a^*) = \exp(-\sigma/\alpha)\,\delta(V^*) + \pi^{-3/2} \int_0^{\sigma/\alpha} \mathrm{d}s_1 \exp(-s_1) \exp(a^{*2}\eta^* s_1) \times \exp(a^* s_1 V_y^* \partial/\partial V_x^*) \exp[-\exp(\tfrac{2}{3} a^{*2}\eta^* s_1)\, V^{*2}]\,, \tag{4.32}$$

where we have performed the change $\sigma' \to s_1 = (\sigma - \sigma')/\alpha$. Similarly, eq. (4.25) becomes

$$\eta^*(a^*) = \int_0^{\sigma/\alpha} \mathrm{d}s_1\, s_1 \exp[-(1 + \tfrac{2}{3} a^{*2}\eta^*) s_1] = \frac{1}{(1 + \frac{2}{3} a^{*2}\eta^*)^2} \{1 - \exp[-(1 + \tfrac{2}{3} a^{*2}\eta^*)\sigma/\alpha] \times [1 + (1 + \tfrac{2}{3} a^{*2}\eta^*)\sigma/\alpha]\}\,. \tag{4.33}$$

Eq. (4.33) is still a very difficult implicit equation for $\eta^*(a^*)$. Consequently, the a^*-dependence in eq. (4.32) is still very involved. On the other hand, we have already seen that $\eta^*(a^*)$ and $\sigma^*(a^*)$ are rather insensitive to the value of α. Thus, our second step consists of replacing the functions $\eta^*(a^*)$ and $\sigma^*(a^*)$ appearing on the right sides of eqs. (4.32) and (4.33) by the ones corresponding to Maxwell molecules, as given by eqs. (3.11) and (4.23). Therefore, one finally gets

$$f^*(V^*; a^*) = \exp(-\sigma_{\mathrm{M}}/\alpha)\,\delta(V^*) + \pi^{-3/2} \int_0^{\sigma_{\mathrm{M}}/\alpha} \mathrm{d}s_1 \exp(-s_1) \times \exp(\tfrac{3}{2}\lambda^* s_1) \exp(a^* s_1 V_y^* \partial/\partial V_x^*) \exp[-\exp(\lambda^* s_1) V^{*2}]\,, \tag{4.34}$$

$$\eta^*(a^*) = \frac{3}{2}\frac{\lambda^*}{a^{*2}}\{1-\exp[-(1+\lambda^*)\sigma_M/\alpha]\,[1+(1+\lambda^*)\sigma_M/\alpha]\}\,. \qquad (4.35)$$

Several comments about these equations are in order. Eqs. (4.34) and (4.35) are nothing but gross caricatures of eqs. (4.20) and (4.25), respectively. Due to the inconsistency of keeping finite the upper limit in the integrals of eqs. (4.32) and (4.33) and, however, not including higher order terms in eqs. (4.30) and (4.31), eqs. (4.34) and (4.35) cannot be justified from a rigorous mathematical point of view, even for small α. In this respect, it is worth mentioning that eq. (4.34) verifies the conditions (2.16) and (2.17), is consistent with eq. (4.35), but does not satisfy eq. (2.18).

The main advantage of eqs. (4.34) and (4.35) is that they exhibit an explicit dependence on both a^* and α. Since $\sigma_M \simeq \frac{3}{4}a^{*-2}$ for small a^*, it is evident that the functions f^* and η^* given by eqs. (4.34) and (4.35) present an essential singularity at $a^*=0$. Seen as functions of α, they also have an essential singularity at $\alpha=0$. Both singularities are coupled. In the limit $\alpha\to 0^+$, eqs. (4.34) and (4.35) become eqs. (3.24) and (3.11), respectively, which are regular at $a^*=0$. All these features are expected to hold also for the exact expressions (4.20) and (4.25).

The model shear viscosity given by eq. (4.35) for $\alpha = 1/2$ is plotted in fig. 5. The model VDF given by eq. (4.34) is also plotted in figs. 9–12. We observe that, while the model is hardly distinguishable from the case of Maxwell molecules for intermediate and small values of a^*, it is much closer to hard spheres for large values of a^*. This shows the usefulness of eq. (4.34) not only to isolate the main qualitative features of eq. (4.20), but also to give decent quantitative estimates.

5. Conclusions

The exact solution of the BGK equation for a system under (time-dependent) uniform shear flow (USF) has been obtained and analyzed in this paper. This state is spatially uniform in the Lagrangian frame of reference and is characterized by only one nonequilibrium parameter: the reduced shear rate a^*. These advantages, along with the mathematical simplicity of the BGK kinetic equation, allow a quite detailed study of situations arbitrarily far from equilibrium. Special attention has been paid to the velocity distribution function (VDF) itself, rather than only to the transport coefficients. Moreover, the influence of the interaction potential has been monitored for potentials of the form $V(r)\sim r^{-l}$ through the parameter $\alpha = 1/2 - 2/l$, ranging from 0 to 1/2. The following points summarize the most important conclusions and their relationship to the questions raised in section 1.

1) For sufficiently long times, the system reaches a hydrodynamic regime, even far from equilibrium. "Hydrodynamic" is understood here as "independent of the initial conditions". Except in the case of Maxwell molecules, this is achieved after a finite number of collisions. If the conventional criterion of infinitely many collision times is imposed, the hydrodynamic regime is restricted to states close to equilibrium. This distinction between a strong criterion and a weak one is related to viscous heating effects and does not apply for situations where the system eventually reaches a steady state.

2) The Chapman–Enskog (CE) method provides a representation of the normal solution in the form of a series that, in general, is only asymptotic. The exception corresponds again to Maxwell molecules, where the CE series is convergent.

3) The state of the system is highly distorted far from equilibrium. Some of the qualitative features could be anticipated on the basis of the first few terms of the CE expansion. On the other hand, highly nonlinear effects that are not present in the CE expansion, such as the divergence of the VDF at zero velocity, emerge for large shear rates.

4) Even near local equilibrium, there exists a substantial formal difference between the VDFs for Maxwell molecules and for more general repulsive interactions. In the latter case, a Dirac delta term around zero velocity appears. The amplitude of this term is the fraction of particles that have not collided yet since the infinitely remote initial time. This amplitude vanishes if the strong criterion referred to in point 1 is applied.

5) Nonetheless, the transport properties, such as the shear viscosity, are relatively insensitive to the details of the potential when they are properly scaled. The fact that an expansion in powers of the shear rate is convergent only for Maxwell molecules does not seem to have a quantitative effect.

6) Finally, a lot of caution is needed when extending some of the above conclusions to other nonequilibrium states. For instance, the singular role played by Maxwell molecules and the existence of the delta term are essentially due to the peculiarities of the USF and the viscous heating effects associated to it. Previous studies of stationary nonequilibrium states [22] do not exhibit some of these features. On the other hand, the divergence of the CE series and the distortion of the VDF far from equilibrium seem to be much more general properties.

Acknowledgments

Partial support from the Dirección General de Investigación Cientifica y Técnica (Spain) through grants Nos. PS 89-0183 (A.S.) and PB 86-0205 (J.J.B.) is gratefully acknowledged.

Appendix A

In this appendix, the result (3.22) is derived. Since $T(t)/T_0 \to \infty$ when $t - t_0 \to \infty$, eq. (3.22) is equivalent to

$$\lim_{\gamma\to\infty} \gamma^3 g(\gamma\boldsymbol{\xi}) = \delta(\boldsymbol{\xi}) , \tag{A.1}$$

where $g(\boldsymbol{\xi})$ is an arbitrary function subject to the following normalization conditions (cf. eqs. (2.16)–(2.18)):

$$\int d\boldsymbol{\xi}\ g(\boldsymbol{\xi}) = 1 , \tag{A.2}$$

$$\int d\boldsymbol{\xi}\ \boldsymbol{\xi} g(\boldsymbol{\xi}) = 0 , \tag{A.3}$$

$$\int d\boldsymbol{\xi}\ \xi^2 g(\boldsymbol{\xi}) = \tfrac{3}{2} . \tag{A.4}$$

If we define

$$G(\boldsymbol{\xi};\gamma) \equiv \gamma^3 g(\gamma\boldsymbol{\xi}) , \tag{A.5}$$

eqs. (A.2)–(A.4) become

$$\int d\boldsymbol{\xi}\ G(\boldsymbol{\xi};\gamma) = 1 , \tag{A.6}$$

$$\int d\boldsymbol{\xi}\ \boldsymbol{\xi} G(\boldsymbol{\xi};\gamma) = 0 , \tag{A.7}$$

$$\int d\boldsymbol{\xi}\ \xi^2 G(\boldsymbol{\xi};\gamma) = \tfrac{3}{2}\gamma^{-2} . \tag{A.8}$$

In the limit $\gamma\to\infty$, $G(\boldsymbol{\xi};\gamma)$ becomes a function with unit norm and vanishing first moments. Consequently,

$$\lim_{\gamma\to\infty} G(\boldsymbol{\xi};\gamma) = \delta(\boldsymbol{\xi}) \tag{A.9}$$

with independence of the detailed form of $g(\boldsymbol{\xi})$. Notice that $G(\boldsymbol{\xi};\gamma)$ is obtained from $g(\boldsymbol{\xi})$ by shrinking the three components of $\boldsymbol{\xi}$ by a factor of γ and, at the same time, scaling the function to preserve the norm. As $\gamma\to\infty$, the whole function $g(\boldsymbol{\xi})$ is concentrated around a vanishing neighborhood of $\boldsymbol{\xi} = \boldsymbol{0}$.

As an illustration, let us assume that $g(\boldsymbol{\xi})$ is a Gaussian:

$$g(\boldsymbol{\xi}) = \pi^{-3/2} \exp(-\xi^2) . \tag{A.10}$$

Then,

$$G(\boldsymbol{\xi}; \gamma) = \pi^{-3/2} \gamma^3 \exp(-\gamma^2 \xi^2) \tag{A.11}$$

and eq. (A.9) clearly holds.

Appendix B

Some properties of the incomplete gamma function will be derived in this appendix. First, define the function

$$F(x, \varepsilon) \equiv \Gamma(x, \varepsilon) + \sum_{k=0}^{\infty} \frac{(-1)^k}{k!} \frac{1}{k+x} \varepsilon^{k+x} , \tag{B.1}$$

which is convergent for any x and (positive) ε. Insertion of the recurrence relation [18]

$$\Gamma(x, \varepsilon) = \varepsilon^{x-1} \exp(-\varepsilon) + (x-1)\Gamma(x-1, \varepsilon) \tag{B.2}$$

into eq. (B.1) yields

$$F(x, \varepsilon) = (x-1)F(x-1, \varepsilon) . \tag{B.3}$$

Another important property of the function $F(x, \varepsilon)$ is that it does not depend on ε:

$$\frac{\partial F(x, \varepsilon)}{\partial \varepsilon} = -\varepsilon^{x-1} \exp(-\varepsilon) + \varepsilon^{x-1} \sum_{k=0}^{\infty} \frac{(-1)^k}{k!} \varepsilon^k = 0 . \tag{B.4}$$

Therefore, $F(x, \varepsilon) = \lim_{\varepsilon \to 0+} F(x, \varepsilon)$. By taking this limit in eq. (B.1) for $x > 0$, we get

$$F(x, \varepsilon) = \Gamma(x) , \tag{B.5}$$

where $\Gamma(x) \equiv \Gamma(x, 0)$ is given by the integral (3.32) with $\varepsilon = 0$. Such an integral does not exist if $x < 0$. However, $\Gamma(x)$ still can be defined (except for $x = 0, -1, -2, \ldots$) as an analytic continuation by means of the recurrence

relation $\Gamma(x) = (x-1)\Gamma(x-1)$. Since this relation coincides with eq. (B.3), we conclude that eq. (B.5) holds for any x different from a non-positive integer. With that exception in mind, eqs. (B.1) and (B.5) yield

$$\Gamma(x, \varepsilon) = \Gamma(x) - \sum_{k=0}^{\infty} \frac{(-1)^k}{k!} \frac{1}{k+x} \varepsilon^{k+x}. \tag{B.6}$$

Let us now take the limit $x \to 0$. Eq. (B.6) can be rewritten as

$$\Gamma(x, \varepsilon) = \frac{1}{x}\left(\Gamma(x+1) - \sum_{k=0}^{\infty} \frac{(-1)^k}{k!} \frac{\varepsilon^{k+x+1}}{k+x+1} - \varepsilon^x e^{-\varepsilon}\right), \tag{B.7}$$

where use has been made of eq. (B.2). Application of L'Hôpital's rule yields

$$\Gamma(0, \varepsilon) = -\gamma_E - \ln \varepsilon - \sum_{k=1}^{\infty} \frac{(-1)^k}{k!} \frac{\varepsilon^k}{k}, \tag{B.8}$$

where $\gamma_E = -\Gamma'(1)$ is Euler's constant. Repeated application of eq. (B.2) allows one to get $\Gamma(x, \varepsilon)$ from $\Gamma(0, \varepsilon)$ when $x = -n$ is a negative integer. The result is

$$\Gamma(-n, \varepsilon) = \frac{1}{n!}\left[(-1)^n \Gamma(0, \varepsilon) + \exp(-\varepsilon) \sum_{k=0}^{n-1} (-1)^k (n-1-k)! \varepsilon^{n-1-k}\right]. \tag{B.9}$$

Eqs. (B.6), (B.8), and (B.9) give useful representations of the incomplete gamma function for all values of x and $\varepsilon > 0$. In the limit $\varepsilon \to 0^+$, we have

$$\Gamma(x, \varepsilon) \approx \begin{cases} \Gamma(x), & x > 0, \qquad \text{(B.10)} \\ -\dfrac{\varepsilon^x}{x}, & x < 0, \qquad \text{(B.11)} \end{cases}$$

$$\Gamma(0, \varepsilon) \approx -\ln \varepsilon. \tag{B.12}$$

Appendix C

The consistency of the asymptotic behavior

$$|c_k| \sim r^k k! \tag{C.1}$$

for the coefficients of the expansion (4.5) will be shown in this appendix. Let

us get first the recursive relation for those coefficients. Eq. (4.5) gives

$$\frac{\partial \eta^*}{\partial z} = \sum_{k=0}^{\infty} c'_k z^k , \qquad c'_k \equiv (k+1)c_{k+1} , \tag{C.2}$$

$$\frac{\partial^2 \eta^*}{\partial z^2} = \sum_{k=0}^{\infty} c''_k z^k , \qquad c''_k \equiv (k+1)c'_{k+1} = (k+1)(k+2)c_{k+2} . \tag{C.3}$$

Inserting eqs. (4.5), (C.1), and (C.2) into eq. (4.1), one gets

$$\begin{aligned} c_k = &-\tfrac{16}{9}\alpha^2[(c''(cc))_{k-4} + (c(c'c'))_{k-4}] + \tfrac{8}{3}\alpha(cc')_{k-2} \\ &+ \tfrac{16}{3}\alpha(\tfrac{1}{2}-\alpha)(c(cc'))_{k-3} - \tfrac{2}{3}(2-\alpha)(cc)_{k-1} \\ &- \tfrac{8}{9}(\tfrac{1}{2}-\alpha)(1-\alpha)(c(cc))_{k-2} , \qquad k \geq 4 , \end{aligned} \tag{C.4}$$

where we have introduced the short-hand notation

$$(ab)_k \equiv \sum_{m=0}^{k} a_{k-m} b_m = \sum_{m=0}^{k} b_{k-m} a_m \tag{C.5}$$

for the expansion coefficients of the product of two functions whose coefficients are a_k and b_k, respectively. Now, if the behavior (C.1) is assumed, c_k grows so rapidly that the summations of the form (C.5) can be replaced by its largest term. For instance,

$$\begin{aligned} \frac{1}{2|c_k|}\,|(cc)_k - 2c_k| &\leq \frac{1}{2|c_k|}\left(\sum_{m=0}^{k} |c_{k-m}|\,|c_m| - 2|c_k|\right) \\ &\sim \frac{1}{2}\sum_{m=0}^{k} \frac{(k-m)!m!}{k!} - 1 \\ &= \frac{k+1}{2}\sum_{m=0}^{k} \int_0^{\infty} dx\, \frac{x^m}{(1+x)^{k+2}} - 1 \\ &= (k+1)\int_0^1 dx\, \frac{1-x^{k+1}}{1-x^2}\exp[-(k+1)\ln(1+x)] - 1 \\ &= k^{-1} + 2k^{-2} + 8k^{-3} + \mathcal{O}(k^{-4}) . \end{aligned} \tag{C.6}$$

Similarly,

$$(cc')_k \sim (k+1)c_{k+1} \sim r^{-1}c_{k+2} . \tag{C.7}$$

$$(c'c')_k \sim 2(k+1)c_1 c_{k+1}\,, \tag{C.8}$$

$$(c(cc))_k \sim 3c_k\,, \tag{C.9}$$

$$(c(cc'))_k \sim (k+1)c_{k+1} \sim r^{-1}c_{k+2}\,, \tag{C.10}$$

$$(c(c'c'))_k \sim 2(k+1)c_1 c_{k+1} \sim 2r^{-1}c_1 c_{k+2}\,, \tag{C.11}$$

$$(c''(cc))_k \sim (k+1)(k+2)c_{k+2} \sim r^{-2}c_{k+4}\,. \tag{C.12}$$

Consequently, the dominant terms in eq. (C.4) are

$$c_k = -\tfrac{16}{9}\alpha^2 r^{-2}c_k + \tfrac{8}{3}\alpha r^{-1}c_k\,, \tag{C.13}$$

which implies

$$r = \tfrac{4}{3}\alpha\,. \tag{C.14}$$

Appendix D

The function $\sigma(a^*)$ for Maxwell molecules is derived in this appendix. Let us rewrite eq. (4.21) as

$$\frac{\partial\sigma}{\partial z} = -\frac{3}{4}\frac{1}{z^2\eta^*} = -\frac{1}{3}\frac{1}{\lambda^{*2}(1+\lambda^*)^2}\,, \tag{D.1}$$

where $z \equiv a^{*2}$ and use has been made of eqs. (3.3) and (3.11) in the last step. From eq. (3.3) one also has

$$\frac{\partial z}{\partial\lambda^*} = \tfrac{3}{2}(1+\lambda^*)(1+3\lambda^*)\,. \tag{D.2}$$

Therefore, eq. (D.1) becomes

$$\frac{\partial\sigma}{\partial\lambda^*} = -\frac{1}{2}\frac{1+3\lambda^*}{\lambda^{*2}(1+\lambda^*)^2}\,. \tag{D.3}$$

The solution of eq. (D.3) with the condition $\sigma(\lambda^* \to \infty) = 0$ is

$$\sigma = \tfrac{1}{2}\lambda^{*-1} + \ln(1+\lambda^{*-1})\,. \tag{D.4}$$

References

[1] J.A. McLennan, Introduction to Nonequilibrium Statistical Mechanics (Prentice-Hall, Englewood Cliffs, NJ, 1989).
[2] H.J.M. Hanley, ed., Nonlinear Fluid Behavior (North-Holland, Amsterdam, 1983).
[3] W.G. Hoover, Annu. Rev. Phys. Chem. 34 (1983) 103.
D.J. Evans and G.P. Morriss, Comput. Phys. Rep. 1 (1984) 299.
[4] J.W. Dufty, A. Santos, J.J. Brey and R.F. Rodríguez, Phys. Rev. A 33 (1986) 459.
[5] J.W. Dufty, J.J. Brey and A. Santos, in: Molecular-Dynamics Simulation of Statistical-Mechanical Systems, G. Ciccotti and W.G. Hoover, eds. (North-Holland, Amsterdam, 1986) pp. 294–303.
[6] J.R. Dorfman and H. van Beijeren, in: Statistical Mechanics, Part B: Time-Dependent Processes, B.J. Berne, ed. (Plenum, New York, 1977) pp. 65–179.
[7] S. Chapman and T.G. Cowling, The Mathematical Theory of Non-Uniform Gases (Cambridge Univ. Press, Cambridge, 1970).
[8] H. Grad, Phys. Fluids 6 (1963) 147.
[9] J. Erpenbeck, Phys. Rev. Lett. 52 (1984) 1333.
[10] J. Gómez Ordóñez, J.J. Brey and A. Santos, Phys. Rev. A 39 (1989) 3038; 41 (1990) 810.
[11] K. Kawasaki and J.D. Gunton, Phys. Rev. A 8 (1972) 2048.
[12] R. Zwanzig, J. Chem. Phys. 71 (1979) 4416.
[13] J.W. Dufty and J.M. Lindenfeld, J. Stat. Phys. 20 (1979) 259.
M.C. Marchetti and J.W. Dufty, J. Stat. Phys. 32 (1983) 255.
J.W. Dufty, Phys. Rev. A 30 (1984) 1465.
[14] V. Garzó, A. Santos and J.J. Brey, Physica A 163 (1990) 651.
[15] E. Ikenberry and C. Truesdell, J. Rat. Mech. Anal. 5 (1956) 55.
C. Truesdell and R.G. Muncaster, Fundamentals of Maxwell's Kinetic Theory of a Simple Monatomic Gas (Academic Press, New York, 1980).
[16] C. Cercignani, The Boltzmann Equation and Its Applications (Springer, New York, 1988).
[17] C.S. Kim and J.W. Dufty, Phys. Rev. A 40 (1989) 6723.
[18] M. Abramowitz and I. Stegun, Handbook of Mathematical Functions (Dover, New York, 1965).
[19] J.J. Brey and A. Santos, unpublished.
[20] A. Santos, J.J. Brey and J.W. Dufty, Phys. Rev. Lett. 56 (1986) 1571.
[21] T. Naitoh and S. Ono, J. Chem. Phys. 70 (1979) 4515.
[22] A. Santos, J.J. Brey and V. Garzó, Phys. Rev. A 34 (1986) 5047.
J.J. Brey, A. Santos and J.W. Dufty, Phys. Rev. A 36 (1987) 2842.
A. Santos, J.J. Brey, C.S. Kim and J.W. Dufty, Phys. Rev. A 39 (1989) 320.
C.S. Kim, J.W. Dufty, A. Santos and J.J. Brey, Phys. Rev. A 40 (1989) 7165.